JPRS-CST-88-017
14 SEPTEMBER 1988

294049

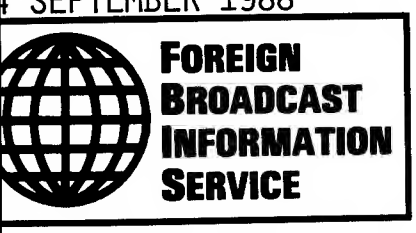

JPRS Report

Science & Technology

China

JPRS-CST-88-017

14 SEPTEMBER 1988

SCIENCE & TECHNOLOGY

CHINA

CONTENTS

/7310

Young Researchers Opting for Foreign Study

40100036 Beijing XINHUA in English 0637 GMT 3 Aug 88

[Text] Bijing, August 3 (XINHUA)--No competition, difficulties in job transfers, and talent being neglected is causing discontent from among young staff members employed by China's research institutes.

According to today's "GUANGMING DAILY," China's young researchers are not doing research, but instead are applying to graduate programs abroad.

"I wanted to work at the Academy of Sciences only because it would give a better chance to study abroad," said one young researcher, adding that ten masters degree holders were assigned to the Academy of Sciences during the past few years, but now, they are all studying abroad.

Dropping out of school, which was once considered a disgrace, is now common at the academy's Bio-Physics Institute.

In the past, talented young people were upset if they failed entrance exams for Chinese graduate programs, but this year, only four applied for 15 graduate positions at China's Acoustics Institute.

Now, because their main goal is to study abroad, young researchers are more eager to get involved in profitable business activities.

"We do not want to follow in the footsteps of those professors whose monthly salary is only enough to buy ten chickens," said one graduate.

"If we don't do more for the younger generation of scientists to take over the lead, in five years China will face a shortage of research personnel," said Zhou Guangzhao, president of China's Science Academy.

"Making the best use of the country's young talent is not only the responsibility of the research institutes, but also the whole society's problem," said Wang Shurong, director of the academy's Physics institute.

According to Wang, there are not enough young people working in the country's key research institutes. According to statistics, the average age of the academy's Bio-Physics Institute's 544-member staff is 45, where in the U.S.-Based Bell Laboratories, the average age is only 33.

In another survey done by the State Education Commission on 8.25 million research workers, those under 30 account for 31 percent, those between 30 and 40 make up 25 percent, and those over 40 involve 44 percent.

New Type Deformation Induced Maraging Stainless Steel Developed

40080157 Tianjin TIANJIN DAXUE XUEBAO [JOURNAL OF TIANJIN UNIVERSITY] in Chinese No 2, Apr 88 pp 39-46

[Article by Li Guojun [2621 0948 0193], Chen Fumin [7115 1788 3046], Yao Jiaxin [1202], Qian Tiangang [6929 1131 0474], and Gao Houxiu [7559 0683 4423] of the Department of Materials Science and Technology, Tianjin University, and Qin Shiqi [4440 0013 7784] of the Tianjin Electric Alloys Plant. Manuscript received 8 Dec 86.]

[Text] Abstract: A new type of deformation induced maraging stainless steel OOCr12-Ni5Mn8Cu2TiRE was developed on the principles of deformation induced martensitic transformation and maraging. The heat treatment of the steel is as follows: 1050°C 0.5h solution treatment + 80 pct cold deformation + 410°C 2.5h aging. It was found that the steel has excellent mechanical properties ($\sigma_b \geqslant 2100$ MPa, $\psi \geqslant 35$ percent, $\delta \geqslant 4$ percent) and good corrosion resistance. There are two kinds of deformation induced martensite, ε and α', and the latter is mainly formed during a larger degree of cold deformation. By analyzing the relationship among tensile strength, degree of cold deformation, the amount of main alloying elements, and the volume fraction of α' martensite, an experimental formula of tensile strength was deduced by mathematical calculation.

I. Foreword

The rapid development of modern science and technology and industrial production has increased the demands on stainless steel tremendously. The scope of application is constantly increasing, and new requirements have been placed on the performance and economy of super high strength stainless steel. Maraging stainless steel has attracted a great deal of attention. Maraging strengthening effects of the super low carbon and high nickel martensite provided superior overall performance[1]. They have been widely used in foreign countries[2]. The cost of maraging stainless steel is often higher because of the higher content of high cost elements. Recently in Japan inexpensive stainless steel sheets and wires have been developed in which Ni is replaced by Mn and N and the strengthening is achieved via deformation induced martensite phase transformation[3]. However, maraging has not been exploited in these developments.

2. Experimental Steel

Four compositions were formulated for the development of inexpensive deformation induced martensite phase transformation and maraging strengthening. The materials were melted in ZG25 vacuum induction furnaces. The chemical compositions are listed in Table 1. The carbon content of #2 steel was made slightly higher than that of #1 steel in order to study the effects of carbon content. Based on the composition of #2 steel, the ratio of Mn and Ni was changed to make #3 and #4 steel. Al and Ti were also added into #4 steel to investigate maraging.

Table 1. Chemical compositions of Experimental steel (wt percent)

No	C	Cr	Ni	Mn	Cu	Ti	Al	Si	RE
1	0.02	11.76	4.32	8.91	1.98	0.88	--	0.44	≤0.05
2	0.06	11.76	4.10	8.90	1.99	1.08	--	0.43	≤0.05
3	0.05	11.77	5.50	7.89	2.07	0.85	--	0.37	≤0.05
4	0.08	11.87	6.75	6.38	2.01	0.62	0.375	0.34	≤0.05

Wire stock and sheet stock used in the experiments were made from 14kg ingots by diffusion annealing, forging, hot rolling and then cold pulling or cold rolling.

3. Selection of Heat Treatment Parameters

3.1 Phase transformation and recrystallization temperature of experimental steel

Experimentally measured recrystallization temperature of the steel was 700 to 750°C. The transition points are listed in Table 2. As can be seen, the Ms points of all the furnaces were below room temperature and satisfied the design requirements.

Table 2. Phase transformation points (°C) of the steel

No	A_s	A_f	M_s
1	625	800	-66
2	575	820	-66
3	650	845	-63
4	625	775	-123

3.2 Selection of solid solution temperature

The furnaces were held at 850-1150°C for 0.5h. The specimens were water cooled, followed by hardness, resistivity and grain size measurements. The results are plotted in Figure 1. The criterion for choosing a solid solution temperature is to yield the smallest austenites. The temperatures chosen for the four furnaces were 950°C for #1, 1000°C for #2, 1050°C for #3 and 950°C for #4. After melting and solidifying, the structures were all austenites with trace of ε-martensites.

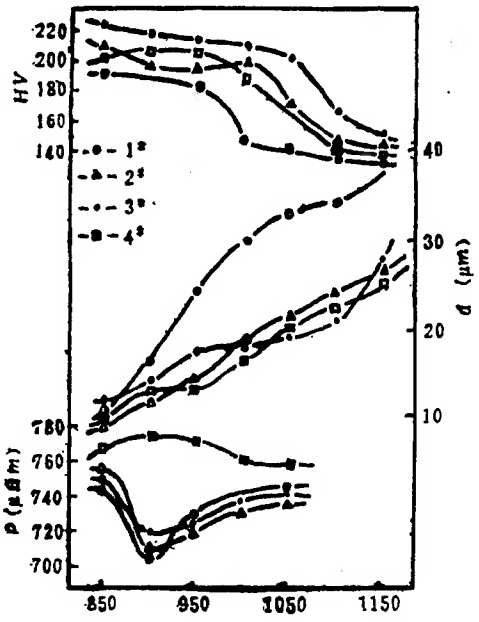

Figure 1. Changes in hardness, resistivity and grain size after solid solution treatments in the four furnaces

3.3 Effects of cold deformation on the structure and performance of the new steels

After solid solution treatments, the new steels were cold deformed to induce martensite transformation. The phase transformation was quite complex. Figure 3 shows the structural changes of the #3 steel under different cold deformations. The figure may be divided into four regions. In region I (deformation of 0-20 percent) the amount of γ phase gradually decreases as deformation increases; ε and α' phases increased slightly. In region II (20-60 percent deformation) γ phase decreases rapidly, ε martensites increase rapidly and the increase of α' is still slow. In region III (60-80 percent deformation), the situation is complex. α' grows rapidly, γ drops slowly and ε decreases rapidly. From the trends, it is anticipated that region IV (>80 percent deformation) will have all three phases approaching constant values.

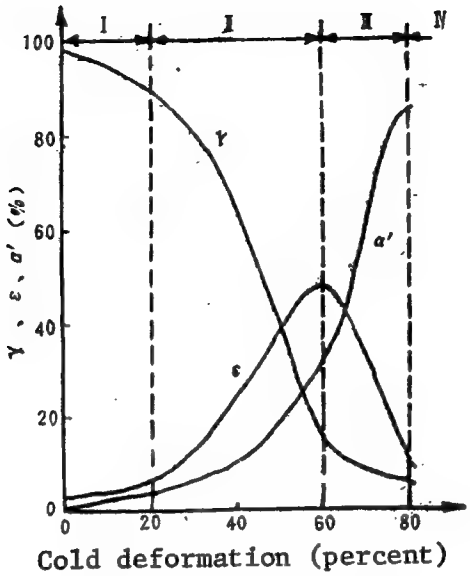

Figure 3. Variations of γ, ε and α' phases of #3 steel under different cold deformations.

The results above show that there are two types of deformation-induced martensites in the new steels; one type is the ε-martensite formed by 0-50 percent deformation that decreases as deformation becomes larger, the other type is α'-martensite formed by deformations greater than 50 percent that increases with deformation and approaches a constant level. Extensive electromicroscope and x-ray diffraction experiments show that the ε-martensite has a hexagonal close-pack structure with internal substructures of dislocations. The structure of α'-martensite is body-centered cubic with internal substructures of high-density dislocations. The α'-martensite provides a good basis for maraging strengthening, which is the goal of this work. Test results show that the optimum cold deformation level is 75-80 percent.

3.4 Parameter selection for maraging process

Samples cold deformed for 80 percent are maraged for 2 hours at 200-530°C and their mechanical properties are then measured. The results show that maraging strengthening at 410°C yields the highest mechanical strength. Table 3 shows the mechanical properties of the steels after 2 hours of maraging at 410°C. The overall mechanical properties of #3 steel are the best.

Table 3. Mechanical properties of steel wires after maraging*

No	Tensile strength σ_b (MPa)	Extension coeff. δ (%)	Cross-section reduction ψ (%)	No of bendings (η)	Hardness (HV)
1	1983	3.6	28	3	559
2	1977	3.5	20	2	549
3	1983	4.0	30	4	472
4	2014	2.0	5	-	560

* Processing steps: Solid solution treatment + 80 percent cold deformation + 2h 410°C maraging.

Maraging curves of wires and sheets that had been through the solid solution treatment and 80 percent deformation are shown in Figure 5. The figure shows that the maximum strength was attained by the #3 steel after 2.5 hours of maraging at 410°C; its mechanical properties are σ = 2150MPa, ψ = 36 percent and δ = 4 percent.

The choices of processing parameters made here are based on strength; for other applications the parameters may be adjusted accordingly.

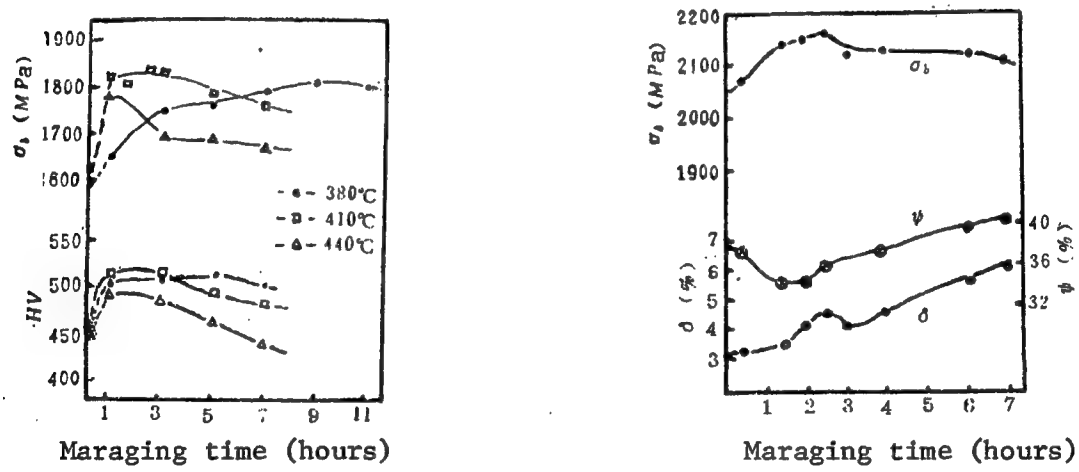

(a) Sheet sample (b) Wire sample maraging at 410°C

Figure 5. Maraging curves of wire and sheet samples of #3 steel after solid solution treatment and 80 percent cold deformation

3.5 Corrosion resistance of the experimental steels

The rate of weight reduction of the test steels was measured in 3 percent NaCl, 50 percent H_2SO_4, and 30 percent HCl and compared with 1Cr18Ni9Ti and 2Cr13. The results are listed in Table 4. The data show that all the experimental steels are much more corrosion resistant than 2Cr13 and are

comparable to 1Cr18Ni19Ti in 50 percent H_2SO_4. In 30 percent HCl solution, all except #4 are better than or comparable to 2Cr13 but worse than 1Cr18Ni19Ti. In 3 percent NaCl solution all samples except #4 are comparable to 2Cr13.

Based on the results above, #3 steel has the best overall properties.

Table 4. Weight loss rate (5) in various media after 200 hours

No	Heat treatment	50%H_2SO_4	30%HCl	3%NaCl
1	Solid solution treatment + 80% cold deformation + 410°C, 2h maraging	19.5	16.8	0.016
2	"	20.5	18.1	0.044
3	"	18.4	29.2	0.065
4	"	19.3	51.6	0.200
2Cr13	Solid solution treatment + 60% cold deformation + low-temperature temper	100	28.6	0.024
1Cr18Ni9Ti	Solid solution + 60% deformation	21.5	8.6	0.017

4. Strengthening mechanism of deformation-induced martensite

There are four strengthening methods in new steels: solid solution strengthening, martensitic strengthening, deformation strengthening, and maraging strengthening. The results of these methods are shown in Table 5. Deformation strengthening refers to the strengthening mechanism accompanying the deformation-induced martensitic transformation. It actually includes strengthening by induced martensitic transformation and by martensitic and austenitic deformation. Data in Table 5 show that the principal strengthening mechanisms in the new steels are deformation-induced martensitic phase transformation and martensitic maraging. The effects of solid solution are small.

Table 5. Strengthening effects in the four new steels

No	Solid solution $\Delta\sigma_b^*$ (MPa)	%	Deformation $\Delta\sigma_b^{**}$ (MPa)	%	Maraging $\Delta\sigma_b^{***}$ (MPa)	%
1	264	13.3	778	40.0	661	33.0
2	341	17.2	707	35.7	651	33.0
3	282	14.2	894	45.0	526	26.5
4	296	14.8	703	35.0	731	36.6

* The strength of solid solution not containing C, Ni, and Mn is assumed to be 280MPa.

** Cold deformation was 75 percent.

*** Maraging at 410°C for 2 hours.

All percentages in table above are for the increase in strength.

We shall now first analyze the effects of alloying on solid solution strengthening. In terms of chemical composition, #2 steel has a slightly higher content of carbon than #1 steel and the difference in solid solutions is mainly caused by carbon. The carbon contents of #3 and #2 steels are comparable and the differences in the strength of the two solid solutions are caused mainly by the fraction of Mn and Ni. Mathematical analyses lead to the following empirical equation:

$$\sigma_b(\text{MPa}) \text{ solid solution} = 1800(C) + 17(Mn - Ni) + 430 \quad (1)$$

where the chemical symbols are in weight percents.

In deformation strengthening by induced martensitic transformation, increases in alloying elements can on the one hand increase the strength and work hardening of the deformation-induced martensites, and on the other hand effect the rate of formation and amount of deformation-induced martensites. This leads to an increase in strength of the deformed steel. The effects of alloying are therefore complex. The following equation is an empirical formula for the increase in tensile strength in steel cold deformed to 75-80 percent:

$$\Delta\sigma_b(\text{MPa}), \text{ deformation} = 900 + 20\,(\varepsilon - 75) + 69200\,(C-0.046)^2 - 2743\,(Ni/Mn - 0.74)^2 \quad (2)$$

where ε is the cold deformation in percent and the chemical symbols are the weight percents of the elements.

By comparing the maraging effects listed in Table 5, #4 steel produced the best results. This indicates that the composite addition of Al and Ti leads to good maraging effect. It should be pointed out, however, that the differences in maraging results are caused mainly by the differences in the volume fraction of α'-martensites. Analysis of the data produced

the following empirical equation for the tensile strength increment $\Delta\sigma_b$ due to maraging:

$$\Delta\sigma_b \text{ maraging (MPa)} = 700 - 18000\, e^{-0.0665V_{\alpha'}} \qquad (3)$$

where $V_{\alpha'}$ represents the volume fraction of α'-martensites. With composite addition of Al and Ti, the tensile strength can be increased by another 100MPa.

By combining (1), (2) and (3), we obtain an empircal equation that describes the relationship between the tensile strength of deformation-induced martensite maraging stainless steel and the chemical composition, cold deformation, and the volume fraction of α'-martensite:

$$\begin{aligned}\sigma_{b\,(MPa)} = {} & 2030 + 20(\varepsilon - 75) + 1800(C) + 100(Al + Ti)^* \\ & + 69200(C - 0.046)^2 + 17(Mn - Ni) \\ & - 2743(Ni/Mn - 0.74)^2 - 18000e^{-0.0665V_{\alpha'}}\end{aligned} \qquad (4)$$

In (4), * indicates the additional increase of 100MPa when Al and Ti are added. Without an*, this increment is zero.

The range of applicability of (4) is: carbon content $\leqslant$0.2 percent, cold deformation $\geqslant$60 percent, deformation-induced martensite (α') >60 percent, and Ti content (or Al + Ti content) approximately 1 percent. The relative errors in the experimental and computed tensile strengths of the various samples are within 2 percent.

5. Conclusion

1) The new deformation-induced martensite maraging stainless steel has good mechanical properties and corrosion resistance. The heat treatment process is simple and the alloying elements are inexpensive. It can be used in the manufacture of simple shaped super strength components.

2) Among the experimental steels, #3 steel has the best overall properties. Its designation is 00Cr12Ni5Mn8Cu2TiRE. The preferred heat treatment of this steel is 0.5 h solid solution treatment at 1050°C, plus 80 percent cold deformation and followed by 2.5h of maraging at 410°C. After heat treatment, the typical mechanical properties are σ_b = 2100-2200 MPa, δ = 4-6 percent and ψ = 35-40 percent.

3) There are two types of deformation induced martensites, the ε-martensite and the α' martensite with high-density dislocation substructures. A necessary condition for improved mechanical properties is an α'-martensite content of 80 percent or more.

4) The principal strengthening mechanism of the new steel is the deformation strengthening accompanying the phase change of the induced martensite, followed by martensitic maraging.

5) An overall analysis of the various strengthening mechanisms lead to the following empirical relationship for the tensile strength and the chemical composition, cold deformation and α' martensite volume percent:

References

1. Golovinskaya, T. M. et al., IZV. ANSSSR Metally, (1980) 3, 183.

2. Mironenko, P. A. et al., MiTOM, (1980) 4, 47.

3. Gaotian Chongyang, Special Steels, 30 (1981) 10, 31.

4. Angel, T., JISI, 177 (1954), 165.

5. Tamura, I., Met. Sci., 16 (1982), May, 245.

6. Maki, T. et al., J. Soc. Mater. Sci. Jpn., 24 (1975), 150.

9698/9604

STUDY OF NEW TYPE SEMI-LINING ELECTROSLAG REMELTING

40090122a Beijing JINSHU XUEBAO [ACTA METALLURGICA SINICA] in Chinese Vol 24 No 3, Jun 88 pp B155-B162

[English abstract of article by Chen Chongxi [7115 1504 4406], et al., of Beijing University of Iron and Steel Technology]

[Text] A new type of electroslag refining technique has been proposed and the influence of the superimposed DC density on the contents of the active metal elements as well as on the desulphurization and degassing have been studied. The results show that the energy consumption may be reduced by 41 percent when using this technique. During the semi-lining ESR under a normal atmosphere, no evident loss of active metal elements occurs while the O, N and S contents can be effectively reduced to 10 ppm in the GH49 and GH37 superalloys. The ingot solidifies along its axis and has a compact microstructure. The secondary dendrite arm spacing of the semi-lining ESR ingot is about one-third shorter than that of the usual ESR ingot.

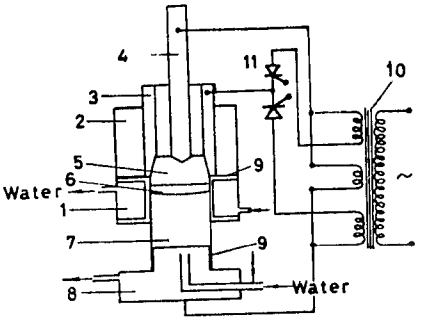

Schematic Diagram of Superimposed DC and Semi-lining ESR Furnace

1. Water-cooled copper crystallizer
2. High temperature resist and heat insulator
3. Superimposed non-consumable circular electrode
4. Consumable metal electrode
5. Slag pool
6. Metal pool
7. Ingot
8. Water cooled base plate
9. High temperature resistant insulated coating
10. Transformer
11. Silicon controlled rectifier

9717

PLASMA CHEMICAL VAPOR DEPOSITED TiN FILMS

40090122b Beijing JINSHU XUEBAO [ACTA METALLURGICA SINICA] in Chinese Vol 24 No 3, Jun 88 pp B163-B168

[English abstract of article by Li Shizhi [2621 0013 4160], et al., of Qingdao Institute of Chemical Technology, Shandong]

[Text] TiN films were deposited onto high speed steel, Si(100) and Si(111) substrates using the DC PCVD method. The crystallographic structure, surface morphology, fracture cross section, microhardness and chlorine content of the PCVD TiN films have been studied. Part of the samples were analyzed using SIMS, AES and ESCA. Experimental results indicate that the structure and properties of the TiN films on different substrates were almost the same when the same deposition parameters were used. At about 500°C, the mode of the film growth underwent a change, probably from layer growth to island growth. The PCVD TiN films had a ratio of N/Ti = 1, and revealed a strong (200) texture. A mixed region existed between the films and the substrates. It can be concluded that PCVD TiN films show good adherence and excellent wear resistant properties and are suitable for anti-friction coating.

9717

Analysis of HBsAg From Different Sources With 5 Anti-A McAbs Against Different Epitopes

40101020 Beijing CHINESE MEDICAL JOURNAL in English Vol 101 No 4, Apr 88 pp 287-291

[Article by Li Zhi-ru, Li He-min, and Hu Zong-han, National Institute for Control of Pharmaceutical and Biological Products, Beijing; notation at bottom of page--"This project is supported by a grant from the National Foundation of Natural Science and from the Ministry of Public Health"]

[Text] Five anti-a monoclonal antibodies (McAbs) were selected and directed to separate epitopes of group a determinant on hepatitis B surface antigen (HBsAg). The method was set up to define the quantitative difference of these epitopes on HBsAg identified by McAbs with ^{125}I-labelled rabbit anti-mouse immunoglobulin antibody (^{125}I-R-M-Ab). The difference of epitope numbers on HBsAg was expressed as epitope density.

Each of the 5 epitopes was of the same density in 3 subtypes of HBsAg (adr, 5 samples; adw, 3; and ay, 4). The average density of the 5 epitopes, identified by McAbs, MHSA 11, 1H9-G11-D7, MHSA 1, 3C1-H7 and 2B8-E8, on the 12 HBsAg samples was expressed as 39 ± 3 percent, 27 ± 2 percent, 17 ±2 percent, 12 ±2 percent, and 6±1 percent, respectively.

The 3 epitope densities identified by MHSA 1, MHSA 11, and 1H9-G11-D7 on yeast derived recombinant HBsAg were statistically different from those on plasm derived HBsAg and cell derived recombinant HBsAg ($P<0.05$). There were some changes of group a determinant between them.

The group a determinant of HBsAg is the main determinant to induce protective antibody for preventing hepatitis B virus infection.[1] It has been found in several laboratories that the group a determinant is very complex and heterogeneous.[2-4] The 2 forms of it, the reduction-resistant and reduction-sensitive form, were proved on HBsAg by alkylation and reduction.[5,6] There are several separate epitopes on it identified with anti-a McAbs.[7-9] Is there any quantitative difference

between these epitopes on HBsAg, or is there any discrepancy between their functions in immune response to hepatitis B virus infection? Our study is an attempt to answer these questions.

Material and Methods

HBsAg samples. 12 HBsAg-positive sera (adr, 5 samples; adw, 3; and ay, 4) were collected by our laboratory. 6 strain recombinant HBsAg vaccines from different companies were provided by our laboratory too, named respectively strain I, II, III, IV, V, and VI. Strains I, II, and III were cell-derived, and strains IV, V, and VI yeast-derived recombinant HBsAg vaccines.

Antibody coated beads. Polystyrens beads, ϕ6.4 mm (Precision Plastic Ball Co. USA) were coated with the solution containing 200 μg/ml purified horse anti-HBs antibody at pH 9.5, 0.05 M sodium carbonate buffer, incubated at 1.5 C for 2 hours, then stored at 4 C overnight. The coated beads were washed with distilled water 3 times, and blocked with 10 percent bovine serum at pH 8.0, 0.01 M phosphate buffer saline at 4 C overnight, washed again, and dried at room temperature.

^{125}I-labelled rabbit anti-mouse immunoglobulin antibody. Rabbit anti-mouse immunoglobulin antibody (Dako Co. Denmark) was iodinated by the chloramine-T method using carrier-free ^{125}I. The rate of ^{125}I to antibody was about 10-30 μci/μg.[10]

RIA kit with ^{125}I-R-M-Ab for HBsAg. The horse antibody coated beads were incubated with 200 μl serial 1:5 dilutions of HBsAg liquid overnight at room temperature, then washed 3 times with distilled water and added with 100 μl of anti-a McAb and ^{125}I-R-M-Ab (80 x 10^4 cpm/100 μl) at room temperature for 4 hours, washed 5 times again, and counted in gamma counter (Beckman 8000, USA).

Results

Separate epitopes identified by anti-a McAbs. 18 anti-a McAbs, provided by several laboratories, were analyzed with the competitive inhibition test and 5 McAbs were selected and directed to separate epitopes of group a determinant on HBsAg.[11] They were MHSA 1, MHSA 11, 2B8-E8, 3C1-H7 and 1H9-G11-D7.

Analysis of epitope densities on HBsAg with ^{125}I-R-M-Ab. The RIA kit with ^{125}I-R-M-Ab was set up and showed parallelism in test for various concentrations of HBsAg in comparison to the RIA kit with ^{125}I-McAb. The kit with ^{125}I-R-M-Ab was superior to the kit with ^{125}I-McAb in methodology. Any McAb could be analyzed of its bound amount to HBsAg with the same batch of ^{125}I-R-M-Ab. The epitopes on HBsAg were bound by McAbs respectively, washed with distilled water to wipe out unbound antibodies and shown bound amount of antibodies to HBsAg with ^{125}I-R-M-Ab. The quantitative differences of epitopes (named epitope

densities) could be determined in the light of the different antibody bound amounts to HBsAg (Table 1).

Table 1. Epitope Densities on HBsAg Anticipated with ^{125}I-R-M-Ab

^{125}I-R-M-Ab	Negative control	5-dilution HBsAg series				
		5^1	5^2	5^3	5^4	5^5
MHSA 1	263	6 777(19%)	7 339(19%)	3 338(18%)	1 499(19%)	581
MHSA 11	271	15 700(44%)	14 828(40%)	7 746(43%)	2 911(39%)	893
2B8-E8	194	1 354(4%)	1 694(4%)	2 064(11%)	506(6%)	281
3C1-H7	237	3 432(11%)	5 072(12%)	753(4%)	1 052(13%)	530
1H9-G11-D7	214	8 462(24%)	9 642(25%)	4 291(23%)	1 769(23%)	611

Note: The percentage in parentheses represents the epitope density.

The bound amounts of 5 McAbs to HBsAg varied as change of the concentration of HBsAg, but the percentage of each antibody bound amount accounting for all 5 antibody bound amounts was almost consistent in the linear range of the kit for 5-dilution HBsAg series. Therefore, the density of each epitope was anticipated according to the formula:

$$A\% = \frac{A_{cpm}}{A_{cpm} + B_{cpm} + C_{cpm} + \cdots} \times 100\%$$

Analysis of 12 HBsAg-positive sera. 12 sera were analyzed by the same method and the density of the epitope identified by MHSA 11 was the highest compared with other 4 epitopes, being 39 ± 3 percent according to the formula. The medium density of epitopes identified by 1H9-G11-D7, MHSA 1, and 3C1-H7 was 27 ±2 percent, 17 ±1 percent, and 12 ± 2 percent, respectively. The low density of the epitope identified by 2B8-E8 was 6 ± 1 percent. There were no obvious variation of the 5 epitope densities among HBsAg subtypes (Table 2).

Table 2. Epitope Densities on HBsAg of 12 Plasm-Positive HBsAg Sera

No.	HBsAg Subtype	Epitope densities on HBsAg (%)				
		MHSA 1	MHSA 11	2B8-E8	3C1-H7	1H9-G11-D7
385	adr	18	38	5	16	24
285	"	18	35	6	17	23
302	"	18	37	4	11	30
521	"	17	35	6	12	30
158	"	16	42	4	11	28
141	adw	17	42	5	10	25
194	"	17	39	7	11	26
402	"	18	37	4	11	28
257	ay	15	37	7	12	29
U 1	"	16	42	5	10	29
U 2	"	16	36	6	12	29
U 3	"	16	42	6	6	29
	Mean	17±1	39±3	6±1	12±2	27±2

Analysis of 6 strain recombinant HBsAg vaccines. The density of 5 epitopes on 6 strain recombinant HBsAg vaccines is shown in Table 3. The densities were different between cell-derived and yeast-derived recombinant HBsAg vaccines. T test of the quantitative differences of each epitope in 3 kinds of HBsAg, plasm-derived HBsAg, cell- and yeast-derived recombinant HBsAg, showed that the density of the 3 epitopes identified by MHSA 1, MHSA 11, and 1H9-G11-D7, on yeast-derived recombinant HBsAg was statistically different from that on plasm-derived HBsAg and cell derived recombinant HBsAg (Table 4).

Table 3. Epitope Densities on Recombinant HBsAg Vaccine

No.	Character	Epitope densities on HBsAg (%)				
		HMSA 1	MHSA 11	2B8-E8	3C1-H7	1H9-G11-D7
I	Cell-derived	19	45	6	11	19
II	Cell-derived	15	46	4	10	23
III	Cell-derived	17	36	4	18	25
	Mean	17±2	42±6	5±1	13±4	22±3
IV	Yeast-derived	10	58	3	15	15
V	Yeast-derived	8	55	8	13	17
VI	Yeast-derived	8	58	7	11	16
	Mean	9±1	57±2	6±3	13±2	16±1

Table 4. Comparative Study of 5 Epitope Densities Between Plasm-Derived HBsAg and Recombinant HBsAg

	Epitope densities on HBsAg (%)				
	MHSA 1	MHSA 11	2B8-E8	3C1-H7	1H9-G11-D7
Plasm-derived HBsAg	17±1	39±3	6±1	12±2	27±2
Cell-derived recombinant HBsAg	17±2	42±6	5±1	13±4	22±3
Yeast-derived recombinant HBsAg	9±1	57±2	6±3	13±2	16±1
T test					
Ppc	—	—	—	—	—
Ppy	0.01	0.01	—	—	0.01
Pcy	0.05	0.05	—	—	0.05

Note: - = no statistical significance, p = plasm, c = cell, y = yeast.

Discussion

There is a direct way for determining the amount of epitopes on antigen. The quantitative difference of epitopes is but anticipated on the basis of different amounts of McAbs bound to the same amount of antigen. Epitopes on antigen are always bound by McAbs in quantities after sufficient incubation without noticeable affection of different affinities of McAbs. According to this principle we have established the method using ^{125}I-R-M-Ab to compare the quantitative differences of several epitopes identified by McAbs on HBsAg. The quantitative differences of epitopes were expressed as epitope densities. Each of the 5 epitopes was of the same density on the 3 HBsAg subtypes. This suggests that the structure of group a determinant on HBsAg of different subtypes was the same. It is good for recipients inoculated with hepatitis B vaccine, because induced antibody against group a determinant could form in them an effective defensive system against infection by hepatitis B virus of different subtypes.[1]

The density of the epitope identified by McAb, MHSA 11, is about 6 times that of the epitope identified by 2B8-E8. The discrepancy between the functions of different epitope densities in immune response to hepatitis B virus infection is still not clear. If the antigenicity and immunogenicity of high epitope density is much stronger than that of low epitope density on HBsAg, the antibody amount induced by high epitope density should account for the large part of the total number of anti-HBs antibodies. About this a concept has already been put forward. According to this concept the high epitope density on antigen should be the strong determinant in inducing the main protective antibodies.

Recombinant hepatitis B vaccine, like plasm-derived hepatitis B vaccine, has been proved to be safe and immunogenic in trials on recipients.[12,13] The study of plasm-derived and recombinant HBsAg vaccines showed statistical difference between the epitope densities, a fact pointing to presence of some changes of the group a determinant on HBsAg. Although statistically significant differences of the total anti-HBs levels have been observed between recipients inoculated respectively with the 2 kinds of hepatitis B vaccines, 14 at present there is yet no convincing evidence to show which of them is better.

References

1. Iwarson S., et al. Neutralisation of hepatitis B virus infectivity by a murine monoclonal antibody: An experimental study in the chimpanzees. J. Med. Virol. 1985; 16:89.

2. Gold, J.W.M., et al. Passive hemagglutination assay for antibody to subtypes of hepatitis B surface antigen. J. Immunol. 1974; 112:1100.

3. Wands, J.R., et al. High affinity monoclonal antibodies to hepatitis B surface antigen produced by somatic cell hybrids. Gastroenterology 1981; 80:225.

4. Courouce, A.M., et al. Monoclonal antibodies to HBsAg: A study of their specificities for eight different HBsAg subtypes. Devel. Biol. Stand. 1983; 54:527.

5. Imai, M., et al. Antigenicity of reduced and alkylated Australia antigen. J. Immunol. 1974; 112:416.

6. Pillot, J., et al. Analysis of the vaccinating group specificity a of HBsAg with monoclonal antibodies: Identification of continuous and discontinuous epitopes. Devel. Biol. Stand. 1984; 57:299.

7. David, G.S., et al. Monoclonal antibodies in the detection of hepatitis infection. Med. Lab. Sci. 1981; 38:341.

8. Goodall, A.H., et al. Monoclonal antibodies in a solid-phase radiometric assay for HBsAg. Med. Lab. Sci. 1981; 38:349.

9. Kennedy, R.C., et al. Characterization of anti-hepatitis B surface antigen monoclonal antibodies. Intervirology 1983; 19:176.

10. Hann, P.W., et al. Immunochemical evaluation of radioiodinated protein A. J. Immunol. Meth. 1984; 72:61.

11. Peterson, D.L. et al. Antigenic structure of HBsAg: Identification "d" subtype determinant by chemical modification and use of monoclonal antibodies. J. Immunol. 1974; 132:920.

12. Dandolos E., et al. Safety and immunogenicity of a recombinant hepatitis B vaccine. J. Med. Virol. 1985; 17:57.

13. Jilg, W., et al. Clinical evaluation of a recombinant hepatitis B vaccine. Lancet. 1984; 2:1174.

14. Yeoh, Ek., et al. A comparative study of recombinant versus plasm vaccine in high risk infants (abstract). London Viral Hepatitis International Symposium, 1987:282.

/09599

Biotechnology Seen To Become Boom Industry

40101008a Beijing XINHUA in English 12 Jul 88

[Text] Beijing, July 12 (XINHUA) -- Bio-Technology is expected to become a booming industry in China.

Bio-tech output by the turn of the century will be 50 to 60 times the level of 1985, say experts working on a state strategy and policy for bio-tech development.

The major new products will include glucose, single-cell protein, new-type enzyme syrup, and microbial pesticides, as well as products related to agricultural production.

More varieties of traditional bio-tech products such as vitamins, antibiotics, alcohol and amino acids, will also be offered by the year 2000, the experts say.

Streamline production is planned for many items ranging from genetically engineered vaccines to fibre fermentation in food production.

/12223

Bacteria Helps Produce Crops

40101008b Beijing XINHUA in English 18 Jul 88

[Text] Beijing, July 18 (XINHUA) -- Chinese researchers at the Beijing Agricultural University have developed bacteria that help yield bigger crops.

The crop-yielding bacteria have been tested with 48 kinds of crops on 3.3 million hectares of land throughout China and the results have been "very encouraging," says Chen Yanxi, a biomedical expert at the university and head of the research group.

He says that last year the crop increases on bacteria-treated lands ranged from 10 percent to 32 percent and totalled 600,000 tons of grains and 300,000 tons of rapeseeds worth 600 million yuan.

At least [words indistinct] this year, Chen said adding that different bacteria are used for different crops.

They have been used for rice, wheat, corn, sweet potatoes, cotton, rapeseeds, beans, soybeans, beets, vegetables, watermelons, apple and orange trees, chinese chestnuts, tea, tobacco and mulberry.

The treatment is easy and cheap, Chen said. Seeds may be dressed with the bacteria or the bacteria may be sprayed onto the crops. The cost is less than three yuan each hectare.

Chen said the bacteria used are parasitic varieties, different from those used in fertilizers and pesticides.

"Some microbials kill plants but some help them grow. We just search for and develop the water," Chen said.

/12223

STUDIES OF INDUCTION OF POLLEN PLANTS FROM HYBRIDS OF THREE GENERA--TRITICUM, AGROPYRON, SECALE

40091061a Beijing YICHUAN XUEBAO [ACTA GENETICA SINICA] in Chinese Vol 15 No 3, Jun 88 pp 161-164

[English abstract of article by Zhuang Jiajun [8369 1367 7486], et al., of the Institute of Genetics, Chinese Academy of Sciences, Beijing]

[Text] Hybridizations were conducted between French hexaploid Triticale and each of the two lines (intermediate types 3 and 5) selected from progenies of the crosses between common wheat (T. aestivum) and Agropyron glaucum. The hybrid seeds were obtained. The characteristics of the F_1 hybrid plants of the two cross combinations were between those of their parents and possessed the characteristics of three parent genera. They were intermediate types. Their anthers were inoculated, and potato-2 basic medium was used for pollen callus induction. Calli were transferred onto the 190-2 medium for the regeneration of pollen plants. A number of pollen plants from the anther culture of three genera hybrids was induced successfully. The chromosome compositions of the pollen plants were identified using the Giemsa banding technique.

9717

IDENTIFICATION OF 1B/1R WHEAT-RYE CHROMOSOME TRANSLOCATION

40091061b Beijing YICHUAN XUEBAO [ACTA GENETICA SINICA] in Chinese Vol 15 No 3, Jun 88 pp 165-169

[English abstract of article by Dong Anshu [5516 1344 2579], et al., of the Agronomy Department, Northwestern Agricultural University, Yangling, Shanxi]

[Text] A genetic analysis was made of the 1B/1R translocation chromosome of winter wheat strain 73(36)9-1 in this study. It was found that root-tip cells of 73(36)9-1 had one pair of satellite chromosomes, while its parents, Ai-Feng No 4 and Lovrin 10, had two and one pair of satellite chromosomes, respectively. It was observed that all the metaphase chromosomes of most PMGs of hybrid F_1[73(36)9-1 x Ai-Feng No 4] paired normally, as did those of hybrid F_1[73(36)9-1 x Lovrin 10], except that two univalents were produced in most PMCs. It was also found that the chromosomes paired well and formed a rod heteromorphic bivalent in the hybrid F_1[73(36)9-1 x CSDT 1BL]. However, 73(36)9-1 generally produced the configuration 20''+1'+t' when test-crossed with CSDT 1BS. This shows that the translocation occurred on the chromosome 1B short arm, and this segment came from the rye chromosome 1RL. In the present paper, the authors also discuss possible causes of the translocation, concluding that it was formed through the reunion of two kinds of telocentrica (1BL and 1RL) following the simultaneous misdivision of two univalent chromosomes (wheat chromosome 1B and rye 1R). Therefore, it can be seen that the winter wheat strain 73(36)9-1 is a spontaenous translocation line.

9717

STUDIES OF HEAD SMUT RESISTANCE OF SORGHUM VARIETIES, ITS INHERITANCE

40091061c Beijing YICHUAN XUEBAO [ACTA GENETICA SINICA] in Chinese Vol 15 No 3, Jun 88 pp 170-173

[English abstract of article by Cao Ruhuai [2580 1172 2849], et al., of the Institute of Crop Germplasm Resources, Shanxi Academy of Agricultural Science, Taiyuan]

[Text] During 1981-1985, 1239 sorghum cultivars were tested for resistance to head smut under artificial inoculation conditions. This work resulted in the selection of some cultivars (lines) that were highly resistant and resistant to this disease. These cultivars may be valuable as sources of resistance to head smut in sorghum breeding programs.

Then, having identified the resistance, 17 cultivars (lines) with different degrees of resistance were used in an inheritable experiment designed with incomplete diallel cross, from which 72 hybrid combinations were obtained. Studies on the inheritance of sorghum heat smut resistance were conducted. The results showed that different sorghum varieties were identified as possessing different ways of inheritance of resistance to head smut. Some varieties possess the characteristic of quantitative character inheritance, while other varieties have qualitative character inheritance. The resistance of cultivars (lines) of quantitative inheritance is mainly controlled by additive genes.

9717

REGENERATION OF FERTILE PLANTS FROM COTYLEDON PROTOPLASTS IN SOLANUM MELONGENA L

40091061d Beijing YICHUAN XUEBAO [ACTA GENETICA SINICA] in Chinese Vol 15 No 3, Jun 88 pp 181-184

[English abstract of article by Li Gengguang [2621 5105 0342], et al., of South China Institute of Botany, Chinese Academy of Sciences, Guangzhou]

[Text] Protoplasts were isolated from cotyledons of eggplant (S. melongena cv Yuanjing) in a solution containing 0.75 percent cellulase R-10, 0.2 percent Hemicellulase Rhozyme and 0.2 percent Pectinase. They were induced to small calli in the medium. Shoots were regenerated from calli on MS agar medium with 2 mg/l KT, 0.005 mg/l NAA, and 2 percent sucrose after 1 month. The shoots which grew to a height of 3-4 cm were rooted in a MS medium with 0.1 mg/l IAA, 1 percent activated charcoal and 2 percent sucrose. Roots appeared in 1 week, followed by complete plantlets. They were then transferred to a mixture of sterilized soil, and grew to blossom and bear fruit.

9717

MAP OF EIGHT RESTRICTION ENDONUCLEASES, STRUCTURE BY ELECTRON MICROSCOPE OF CHINESE HUMAN MITOCHONDRIAL DNA

4009106le Beijing YICHUAN XUEBAO [ACTA GENETICA SINICA] in Chinese Vol 15 No 3, Jun 88 pp 215-222

[English abstract of article by He Lin [6320 2651], et al., of the Department of Biology, Nanjing Railway Medical College]

[Text] Although the complete sequence of human mtDNA, which has mainly been determined from the mtDNA of non-Chinese people, was detected by S. Anderson, et al. (1981), it was not confirmed as representing the mtDNA nucleotide sequence for all humans. Therefore, the authors established a map of eight restriction endonucleases for reference in the genetic research of Chinese human mtDNA before the representative sequence of Chinese human mtDNA was detected. The molecular structure of the mtDNA was also studied by electron microscopy, and a small circular DNA, with a perimeter of approximately 2 μm, was found accidentally. This might play a role in message communications or the onset of senescence between nuclear DNA and mtDNA.

9717

NEW METHOD FOR IN SITU NICK TRANSLATION OF HUMAN METAPHASE CHROMOSOMES

40091061f Beijing YICHUAN XUEBAO [ACTA GENETICA SINICA] in Chinese Vol 15 No 3, Jun 88 pp 223-230

[English abstract of article by Li Guiyuan [2621 2710 3293], et al., of the Cancer Research Laboratory, Hunan Medical College, Changsha]

[Text] The transcribing active regions of the mammalian genome have reportedly been visualized by in situ nick translation of the metaphase or premetaphase chromosomes with ^{3}H-dTTP or biotin-labeled dUTP. In this paper, the authors present a basic fuchsin stain technique for in situ nick-translated chromosomes which have been completely substituted with BrdU. The technique provides the opportunity to distinguish active genes from inactive ones by the special banding pattern of chromosomes. The results also demonstrate that the optimal temperature, time and DNase I concentration for in situ nick translation are 20°C, 10-15 minutes and 2 ng/ml, respectively. The banding pattern revealed by this technique is different from that of G- and R-banding in regard to the number and location of bands on the chromosomes. The DNase I-sensitive bands usually correspond to the dark D-bands or light G-bands, but not all the light G-bands are DNase I-sensitive. They have been designated as reverse D-bands. This technique offers four advantages over conventional detection procedures of in situ nick translation of chromosomes with ^{3}H-dTTP and Bio-dUTP: markedly reducing time for banding, strong reproducibility, simultaneous displaying sister chromatid exchanges and in situ nick-translated bands, providing a method for studying the distribution of BrdU requiring hereditary fragile sites on the in situ nick-translated bands.

9717

NEW SPECIES OF SPIROCHAETA ISOLATED FROM ANAEROBIC DIGESTER FEEDING WITH SOYBEAN CAKE WASTEWATER

40091062a Beijing WEISHENGWU XUEBAO [ACTA MICROBIOLOGICA SINICA] in Chinese Vol 28 No 2, Jun 88 pp 97-101

[English abstract of article by Bai Wenxiang [4101 2429 0742], et al., of the Institute of Microbiology, Chinese Academy of Sciences, Beijing]

[Text] A red pigment-producing, helically shaped, obligate anaerobic bacterium was isolated from soybean cake waste digester using the Hungate anaerobic technique. In a liquid medium, cells actively locomate in straight lines or nearly straight lines, and sometimes flex. Many carbohydrates can be fermented with the main products of acetate, alcohol, CO_2 and H_2. Yeast extract is required for growth. Both NH_4Cl and peptone can be used as the nitrogen source. The optimal temperature for growth is 30-35°C. The optimal NaCl concentration is 0-1.0 percent, with a maximum concentration of 2.0 percent. The G+C mol percent of DNA is 49. According to Bergey's "Manual of Systematic Bacteriology" (Vol 1, 1984), this bacterium obviously belongs to the genus Spirochaeta, but it differs from the Spirochaeta listed in Bergey's manual in several respects. It is designated as a new species of Spirochaeta--Spirochaeta rhodogenes sp. nov.

9717

ESTABLISHMENT OF HYBRIDOMA CELL LINES OF ANTI-K99 (ENTEROTOXIGENIC E. COLI SURFACE ANTIGEN), CHARACTERIZATION OF MONOCLONAL ANTIBODY

40091062b Beijing WEISHENGWU XUEBAO [ACTA MICROBIOLOGICA SINICA] in Chinese Vol 28 No 2, Jun 88 pp 115-120

[English abstract of article by Wang He [3769 3109], et al., of the Laboratory of Molecular Biology, Chinese Academy of Agricultural Sciences, Beijing]

[Text] The establishment of hybridoma cell lines which secrete anti-K99 (enterotoxigenic E. coli surface antigen) monoclonal antibody is described. The high titer of the monoclonal antibody in a supernatant of the cell culture was detected after nearly half a year's culture in vitro. The monoclonal antibody was extensively characterized by ELISA, IFA, RIA (dot immunobinding assay), oucherlony and slide agglutination. The high specificity of the antibody can be used as a standard reagent for diagnosing the diarrhea caused by enterotoxigenic colibacillosis and may provide a means of preventing enterotoxigenic colibacillosis in calves and piglets.

9717

STUDIES OF CELLULASE SYSTEM FROM PENICILLIUM DECUMBENS

40091062c Beijing WEISHENGWU XUEBAO [ACTA MICROBIOLOGICA SINICA] in Chinese Vol 28 No 2, Jun 88 pp 121-130

[English abstract of article by Qu Yinbo [2575 7299 3134], et al., of the Institute of Microbiology, Shandong University, Jinan]

[Text] The components of the Penicillium decumbens cellulase system, one β-1,4-glucosidase, six cellobiohydrolases and eight endo-β-glucanases, were purified by gel filtration, ion exchange and hydrophobic interaction chromatography. Most of them showed homogeneity in the gel electrophoresis with or without SDS. Six of the components showing a wide band on the electrophoresis were fractionated further into two to six subcomponents by CM Bio-gel A ion exchange chromatography. The compositions and properties of the components and sub-components were determined. The cellulase components from various microorganisms were related by statistical analysis of the amino acid compositions using a computer. A post-translation modification hypothesis was been proposed to explain the origin of the multiplicity and microheterogeneity of the cellulase system.

9717

STUDIES OF BREEDING OF L-ARGININE-PRODUCING STRAIN

40091062d Beijing WEISHENGWU XUEBAO [ACTA MICROBIOLOGICA SINICA] in Chinese Vol 28 No 2, Jun 88 pp 131-135

[English abstract of article by Lu Zhiqiang [6424 1807 1730] of the Department of Biology, University of Science and Technology of China, Hefei; Gong Jianhua [7895 1696 5478], et al., of the Institute of Microbiology, Chinese Academy of Sciences, Beijing]

[Text] A L-arginine-producing strain, 971.1, was derived from Corynebacterium crenatum AS 1.542 by stepwise mutagenic treatment with N-methyl-N'-nitro-N-nitrosoguanidine.

The L-arginine producer requires histidine as an essential growth factor and is resistant to sulfaguanidine. It has produced 25.2 mg/ml L-arginine in a medium containing (percent): glucose (12), corn steep liquor (1.5), soybean cake hydrolysate (0.8), $(NH_4)_2SO_4$ (6.5), $K_2HPO_4 \cdot 3H_2O$ (0.1), KH_2PO_4 (0.05), $MgSO_4 \cdot 7H_2O$ (0.04), $CaCO_3$ (3.0), pH 7.0, on a rotary shaker at 30°C for 4 days. This mutant has good stability for L-arginine production.

9717

PROPERTIES OF α-AMINO ACID ESTER HYDROLASE IN INTACT CELL OF PSEUDOMONAS AERUGINOSA

40091062e Beijing WEISHENGWU XUEBAO [ACTA MICROBIOLOGICA SINICA] in Chinese Vol 28 No 2, Jun 88 pp 143-148

[English abstract of article by Kou Xiufen [1379 4423 5358], et al., of the Institute of Microbiology, Chinese Academy of Sciences, Beijing]

[Text] α-Amino acid ester hydrolase in an intact cell of Pseudomonas aeruginosa AS 1.204 catalyzed both the hydrolysis of the α-amino acid ester and the transfer of the acyl group from the amino acid ester to amide nucleophiles. The enzymologic properties during hydrolysis paralleled those during transfer. The optimum pH for both hydrolysis and transfer was 5.2 and the optimum temperature was 40°C.

7-amino-3-deacetoxycephalosporanic acid (7-ADCA) inhibited the hydrolysis of phenyglycine methyl ester (PG-OMe). Therefore, the enzyme in the Pseudomonas aeruginosa intact cell catalyzed the conversion of 7-ADCA and PG-OMe to the corresponding semisynthetic cephalosporins.

9717

STUDIES OF MICROBIAL POLYNUCLEOTIDE PHOSPHORYLASE

40091062f Beijing WEISHENGWU XUEBAO [ACTA MICROBIOLOGICA SINICA] in Chinese
Vol 28 No 2, Jun 88 pp 149-154

[English abstract of article by Xie Botai [6200 0130 3141], et al., of Shaanxi Institute of Microbiology, Xi'an]

[Text] A screening for the production of polynucleotide phosphorylase (PNPase) in bacteria, yeasts and fungi by using polyacrylamide gel electrophoresis has been performed. The results show that PNPase is widely distributed. The molecular weight of the bacterial PNPase is the same as that of E. coli. The PNPase of some strains can be degraded by proteinase during isolation to form multiple forms. Others are hardly affected by proteinase. Some strains are able to secrete the PNPase from the cell and can be used to synthesize poly (I:C).

9717

MOLECULAR ANALYSIS OF R-PLASMIDS HARBORED IN SALMONELLA TYPHIMURIUM EPIDEMICS IN HOSPITAL

40091062g Beijing WEISHENGWU XUEBAO [ACTA MICROBIOLOGICA SINICA] in Chinese Vol 28 No 2, Jun 88 pp 155-160

[English abstract of article by Chen Minjun [7115 3046 6874], et al., of Beijing Union Medical College Hospital, Chinese Academy of Medical Sciences]

[Text] Our purpose in this report is to analyze the R-plasmids and their fragments harbored in Salmonella typhimurium epidemics in hospitals to find their molecular differences. Seven strains were randomly studied from 23 rampant epidemics of S. typhimurium. They were identical in biochemical patterns, with their serotype being O_4Hi. According to MIC results and plasmid fingerprints, the seven strains were arranged into two groups: The first group consisted of five strains that were resistant to penicillin (Pc, >500 μg/ml), Ampicillin (Ap, >500 μg/ml), Cefazolin (Cz, 16 μg/ml), Erythromycin (Er, >500 μg/ml), Chloramphenicol (Cm, 250 μg/ml), Streptomycin (Sm, >500 μg/ml), Kanamycin (Km, >500 μg/ml), and Tetracyclin (Tc, >500 μg/ml). It was proved by a transformation test that the eight resistant genes were on a 139 kb large plasmid p139. The second group consisted of two strains that were resistant to six of the eight antibiotics, but were sensitive to Km and Cz, with MIC 8 μg/ml and 1 μg/ml, respectively. Their genes were on a 121 kb large plasmid p121.

The plasmid p121, which was sensitive to Km and Cz, was 18 kb less than p139. Most of the fragments from these two transformants were identical after cutting by EcoRI and HindIII, but a 24 kb fragment from p121 did not exist in plasmid p139, which had three new fragments: 26, 12.5 and 3.5 kb. This suggests that the 24 kb fragment code for Km and Cz transfers into the 18 kb fragment, which reforms the three new fragments. The plasmids in the first group were not exactly identical, with one proving to be 1 kb longer than the others.

9717

AUXOTROPHIC (Glu^-) MUTANT, QIONGLEI STRAIN, OF GENUS SALMONELLA

40091062h Beijing WEISHENGWU XUEBAO [ACTA MICROBIOLOGICA SINICA] in Chinese Vol 28 No 2, Jun 88 pp 161-166

[English abstract of article by He Xiaoqing [0149 2556 7230], et al., of Jiangxi Hygienic and Anti-epidemic Station, Nanchang; Liang Junxun [2733 0193 0534] of Northwest Plateau Institute of Biology, Chinese Academy of Sciences, Xining]

[Text] Two non-motile Salmonella cultures, MC7 and MC21, biochemically identical, belonging to the C_1O-serogroup, isolated from Rattus flavipectus on Hainan Island and Rattus flavescens on Leizhou Peninsula, respectively, both auxotrophic in glutamic acid defective (Glu^-) and designated as of the Qionglei strain at the authors' suggestion, are reported in this paper.

These two cultures showed poor growth on a meat extract agar and no growth in Davis' minimal medium. Ammonium salts are not utilized as the sole nitrogen source. Testing using 20 amino acids and 5 group B vitamins, the only growth occurred in the minimal medium containing 0.5 mg/ml glutamic acid, while no growth occurred in the medium containing other amino acids and group B vitamins. However, growth did occur in the medium containing the amino acids histidine (aromatic and histidine group), valine (pyruvic group), methionine (aspartic group) and proline (glutamic group). Growth could be promoted by vitamin B_1.

9717

TWO NEW SEROVARS BELONGING TO LEPTOSPIRA HEBDOMADIS SEROGROUP

40091062i Beijing WEISHENGWU XUEBAO [ACTA MICROBIOLOGICA SINICA] in Chinese Vol 28 No 2, Jun 88 pp 167-172

[English abstract of article by Zhang Fangzheng [1728 2455 2973], et al., of Kunming Military Medical Institute]

[Text] Two new serovars in the Leptospira hebdomadis serogroup are reported in this paper. Strain A10 was isolated in Mengla County on 9 July 1962 and strain H27 in Hekou County in August 1964. Both strains were isolated from the blood of patients with leptospirosis. The serovar names Leptospira interrogans serovars yunnan and hekou with reference strains A10 and H27 are proposed.

9717

IDENTIFICATION OF FOUR NEW STRAINS OF LEPTOSPIRA

40091062j Beijing WEISHENGWU XUEBAO [ACTA MICROBIOLOGICA SINICA] in Chinese Vol 28 No 2, Jun 88 pp 173-178

[English abstract of article by Li Cuizhi [2621 5050 5347] of Yunnan Provincial Institute of Epidemic Diseases, Xiaguan; Li Zhaohua [2621 2507 5478], et al., of the National Institute for the Control of Pharmaceutical and Biological Products, Ministry of Health, Beijing]

[Text] This paper reports the taxonomic results of new serovars of local Leptospira isolated from patients and animals in Yunnan Province.

The names of these new serovars and their representative strains have been designated as serovar Mengma strain S590 and serovar Zhenkang strain L82 in the Javanica serogroup; serovar Menglian strain S621 in the pyrogenes serogroup; and serovar Yunxian strain L100 in the Tarassovi serogroup.

9717

NEW SPECIES OF STREPTOMYCES PRODUCING VALIDAMYCIN

40091062k Beijing WEISHENGWU XUEBAO [ACTA MICROBIOLOGICA SINICA] in Chinese
Vol 28 No 2, Jun 88 pp 179-182

[English abstract of article by Shi Weiliang [2457 0251 5328], et al., of the Institute of Agricultural Microbiology, Zhejiang Academy of Agricultural Sciences, Hangzhou]

[Text] The Streptomyces strain 7823 was isolated from soil samples collected from a mulberry plantation in Haining County, Zhejiang Province. Its antibiotics strongly inhibited the growth of Pellicularia sasakii, which causes sheath blight in rice as well as other fungi.

Ordinarily the spore-bearing hyphae of the strain are spiral with one to three curls at their ends. Spores are elliptical, except for a few spherical spores. Irregular warts or short thorns appear on their surfaces. The aerial mycelia are white to gray and the substrate mycelia are yellow to light brown or withered green. But the water soluble pigment is brownish yellow in most of the media tested. The cell wall composition of this strain is of type I. In view of the morphological and cultural characteristics as well as the biochemical properties, strain 7823, in comparison with several relative strains, has been identified as a new species and names Streptomyces hainingensis n. sp. Shi and Yan.

9717

Harbin Polytechnical University Develops "SPIDER" All-Purpose Image Processing Environment

40080183 Beijing JISUANJI SHIJIE [CHINA COMPUTERWORLD] in Chinese No 26, 6 Jul 88 p 1

[Text] The "SPIDER All-Purpose Image Processing Environment," developed by a Harbin Polytechnical University team led by Professor Li Zhongrong [2621 0112 2837], includes an all-purpose image processing software package, and consists of an adaptive discrete cosine transform and vector quantized hybrid code compression system, a textural analysis system, a rule-based image segmentation system, and a standard image base. The software package provides functions such as statistical and textural image analysis, geometric transform and orthogonal transform, image enhancement, edge detection and sharpening, and image geometric correction. Programming modules total over 100. A standard image base with various specific characteristics useful for detecting images has been set up among the systems.

The adaptive discrete cosine transform and vector quantized hybrid code compression system utilizes an original VQ encoder design and code-book organized structure. The system's compression ratio is less than 23--a state-of-the-art level.

The rule-based image segmentation system, utilizing data driving, state matching, a layered control strategy, fuzzy decision theory and fuzzy automatic mechanism theory, is a successful exploration of expert system technology applied to image segmentation. Its segmentation results are good, providing an effective foundation for advancing image analysis and recognition; it is a world-class research achievement.

In scale, performance, and areas of application, the entire SPIDER system fully meets the 1987 year-end predetermined targets for the computer vision elements of the United States' Strategic Computer Development Project (the SC Project), but China's system displays more originality with respect to image code compression, textural analysis, and application of expert system technology to image segmentation. This qualifies [the development of] this system to be a research achievement at a state-of-the-art level.

Greater Correlation of Environmental Protection, Economic Development

40081074 Beijing ZHONGGUO HUANJING BAO in Chinese 21 Apr 88 pp 1-2

[Article by Liu Wen [0491 2429]: "Improve Environmental Protection and Coordinate Development of the Economy and the Environment; Study the Experiences About Environmental Protection Contained in the Seventh NPC 'Government Work Report'"]

[Text] The primary objective in the building of socialism is to satisfy the ever increasing material and cultural needs of the masses. A fine environment is an important aspect of the people's needs, and it is also an important requirement for satisfying the people's needs in other regards. Moreover, with steady socioeconomic development and constant improvement of the people's livelihood, the demand for environmental quality will continue to rise. Therefore, China's government has made improvement of environmental protection a basic national policy. It is a wise policy of both practical and long-range significance that must be diligently carried out.

China's environmental protection endeavors have two emphases, namely the economy and public benefit; therefore, economic benefits, social benefits, and environmental benefits must all be reconciled. If environmental benefits are ignored, this is bound to lead to what Comrade Zhao Ziyang pointed out when he said that since the Third Plenum, many of the (economic) benefits that have followed from this body of policies have been canceled out. Clearly, mobilization of the entire society to strive for full economic benefits, including factors affecting the environment, holds extremely important significance in promoting sustained and consistent socioeconomic development.

The fundamental point in socioeconomic development is increase in social productivity and expansion of the reproduction of material goods. Expansion of the reproduction of material goods is certainly not carried out within a closed system, but has to be intertwined with the material cycle and the movement of energy in the natural world. This requires maintenance of a balance between the need for socioeconomic development and the ability of the natural environment to support it. Some people say that environmental problems are generated by economic development. This is true; however, to say that environmental problems will be naturally solved with further development of the economy is not so. Granted that further development of

the economy will make the solution of environmental problems possible, there is no certainty that it will solve them. Unless appropriate actions are taken, further economic development will only bring further deterioration of the economy in its wake, and will, in turn, delay or damage further economic development. Why was it that the Mayan civilization that thrived and prospered during the long period from B.C. 2000 until the 16th century became a historical thing of the past? Recent analysis of satellite photographs has revealed the mystery, namely that as a result of too great a pursuit of immediate returns, the Mayans used their environmental resources badly. Here in China, why is it that the vast northwestern region has historically supported only 10 percent of the population while 90 percent of the population is concentrated in the southeastern region? One important reason is likewise the destruction of the ecology of the northwestern region. As a practical matter, our large-scale modernization efforts have come up against and have generated numerous environmental problems. If this continues, one must be concerned lest it lead to the generation of a vicious cycle within and between socioeconomic development and development of the natural environment. Therefore, in 1983, the Chinese Government rightly formulated synchronized plans for building the economy, building towns and the country, and building the environment, and adopted an environmental protection policy for synchronized implementation and synchronized development.

With this policy as a guide, China's environmental protection work has scored significant advances in recent years. Nevertheless, we must also clear-headedly realize that current environmental problems are still very serious. Environmental protection tasks such as prevention of environmental pollution, rational development of natural resources for use, and safeguarding the ecological balance are extremely daunting. We must decisively adopt a series of policies and actions that are in keeping with China's national circumstances.

1. Improvement of Environmental Protection Control Work, and Making the Most of Supervisory Functions for Environmental Control

Environmental protection is a major issue affecting the situation as a whole in total socioeconomic development that has been made a part of the national constitution. Acting under the guidance, coordination and supervision of environmental control units, all areas, all sectors, and all trades and industries throughout the country should help build the environment. In order to carry out the duties that the state has assigned them, environmental control units must carry out reforms to change the way they function, giving emphasis to environmental supervision. Environmental control units are neither solely responsible for building the environment nor should they take a direct part in cleaning up the environment (the task of cleaning up the environment being the responsibility of those who polluted and damaged the environment). This certainly does not mean a weakening of their authority, but rather a strengthening of it. For example, though protection of nature is a realm requiring joint action by all sectors concerned to do a good job, there is still plenty of work for environmental control units to do. Not only should units concerned provide overall guidance, organize, coordinate, supervise, and inspect, but they must also examine for approval

environmental impact reports that have been prepared for some large-scale resource development projects, insist that both main project and environmental protection plans be prepared at the same time, that work on them begins at the same time, and that they go into operation at the same time in order to avoid damage to the natural ecology. They must also exercise control over natural preserves under their department's control, and take special care of bases for the propagation of rare plant species. Obviously, if they are to meet requirements for reform and change the way they function, environmental control organizations at all levels will have to make extremely great efforts, do a good job with regard to ideology and work style, organization, rules and regulations, and the quality of personnel.

2. Study of an Environmental Protection Strategy, and Setting Environmental Strategic Goals That Are Consistent With National Circumstances

An environmental strategy is a program founded on complete consideration of population, resources, and development factors, and a thorough familiarity with the laws governing the use of natural resources and economic laws. Such a program will serve as a guide, will be all-encompassing, and will endure for all aspects of social life to ensure a fine living and production environment for the masses of people, and to promote sustained and steady socioeconomic development.

Of paramount importance in the study of strategic goals, strategic emphasis, strategic steps, and strategic actions for environmental production is the setting of environmental strategic goals. When setting strategic goals for environmental protection, it is necessary to consider not only present environmental quality and the outlook for the future, but also to consider what financial and economic resources are available, and the level of science and technology. If goals are set too low, environmental pollution and damage will certainly be difficult to control, or they may even get worse endangering not only the people's health, but also possibly damaging development of the national economy. If goals are set too high, too much investment will be required, and this may likewise adversely affect development of the national economy, which may, in turn, restrict increased investment in the environment. According to forecasts made by students of the problem in China, attainment of the environmental goal of being able to maintain the country's socioeconomic reproduction and coordinated development of natural economic reproduction will require an investment in environmental protection during this century of 0.5 percent of the national income.

An environmental strategy has to be a multilevel, multifaceted totality. Not only is nationwide overall research required, but all regions, sectors and special trades have to study strategic questions pertaining to their own environment.

3. Perfection of Environmental Protection Laws for the Gradual Formation of an Integrated System

State control over the environment will necessitate the use of economic, technical, administrative, and educational methods, with legal methods

playing an especially important role. China's environmental legislation may be divided into four broad categories. First is the provisions regarding environmental protection contained in the national constitution; second is basic laws about environmental protection of an overall nature; third is regulations that have been issued or approved by the State Council; and fourth is provisions pertaining to environmental protection in other laws.

There are, in addition, pertinent detailed rules and regulations drawn up by various areas and sectors. All these kinds of laws should be formulated, improved and perfected as quickly as possible. At the same time, laws must be strictly enforced and the power of these laws must be applied.

A critique of experiences during recent years shows that the legal regulations that have been most effective in China are environmental impact assessment regulations and "three simultaneous" regulations, which reflect a policy of "prevention first"; the system of reporting, registration, and issuance of permits to control damage to the ecology and discharge of pollution; enforcement of the principle of "those who do the polluting do the cleaning up"; the collection of fines for the discharge of pollutants, which plays a major role in the collection of funds for environmental protection; and the promotion of a system of rewards for turning the "three wastes" [waste water, waste gas, and industrial residues] into useful resources for use in multiple ways. All of these have to continue to be enforced and further developed. A system for evaluating industrial enterprise environmental protection norms, and a system for controlling the total volume of pollutants, both of which are in process of being tried out, should be formally promulgated for implementation as quickly as possible.

Environmental standards are the foundation for environmental control and the basis for environmental legislation. They must also be formulated, with the national circumstances of the country in mind, and gradually become part of a complete system.

4. Formulation of Environmental Protection Plans for Completion of the Task of Building the Environment for the Next 5 Years and Longer

Environmental protection plans are command-style regulations for attainment of environmental protection goals and actions to be taken during a specific time period. They are a major integral part of plans for national economic and social development. In his government work report, Premier Li Peng called upon us to treasure and protect natural resources such as the soil, water sources, forests, grasslands, the oceans, and wild plants and animals, and to develop various mineral resources in a sensible way and use them effectively. He particularly called for a strict halt to arbitrary takeovers of cultivated land and the destruction of forests. He vigorously advocated beneficial campaigns for planting trees and growing grass, the greening of cities and the countryside; and he called for actively launching a complete clean up of the city and countryside environment, with emphasis on control of the pollution of the atmosphere and water sources, and improved processing of solid wastes. All of these matters, as well as the prevention and control of noise pollution in cities, must be made a part of rural

planning and plans for the prevention and control of pollution by township and town enterprises. These plans must then be broken down for application level by level, checks and examinations being conducted regularly to ensure compliance.

In order to realize the magnificent goals of socioeconomic development during the primary stage of socialism, environmental control units must use scientific forecasting as a basis for formulating medium long environmental protection plans for the Eighth 5-Year Plan period, for the end of the present century, and for the beginning of the next century, making rolling readjustments as the situation develops to improve their feasibility.

5. Good Performance of Environmental Protection Scientific Research and Monitoring Work To Find Patterns of Environmental Evolution and To Take Corresponding Actions

Doing a better job of building, controlling, and cleaning up the environment requires that science and technology be given first place. There must be steady pioneering and moving ahead in the fields of the natural sciences, social sciences, and overlapping sciences. In the environmental science system as a whole, not only must there be an energetic bolstering of research in the "soft sciences" including environmental economics, environmental philosophy, environmental law, and environmental policies, but attention must also be given to the favorable opportunity afforded by the new technological revolution that is taking place in the world when breakthroughs are being made in the field of engineering techniques. Examples include research on new techniques for the revival and strengthening of the regeneration and appreciation of renewable resources, large area planting of trees and growing of grasses, water conservation, and soil improvement, new techniques for the development, transportation and full use of mineral resources, new production technologies that are pollution free or produce little pollution, pollutant removal and transformation mechanisms, new techniques to improve the pollution intake and self-cleansing capabilities of the environment, and new techniques for making use of the public environment that includes the open seas, the polar regions, and outer space. Also requiring study is new techniques for guarding against and solving new environmental pollution problems and destructive factors that follow in the wake of technological progress.

Environmental monitoring work consists of the scientific testing of the types and concentrations of pollutants in the environment, finding out how they are distributed in time and space, as well as the effect they have on the environment, providing monitoring data promptly for environmental forecasting purposes, and periodically compiling the "Environmental Impact Report" as basic data for use in environmental control and scientific study. Improvement of environmental monitoring efficiency requires the establishment--insofar as the country's financial circumstances, numbers of personnel, and technical capabilities permit--of an environmental monitoring network of a certain density, and the purchase of needed environmental monitoring equipment, as well as efforts to improve its utilization rate.

6. Publicity and Education About Environmental Protection To Raise the Whole Nation's Awareness of the Environment

By increasing the whole nation's awareness is meant raising consciousness about protecting and improving environmental quality from the leaders of the country at the top down to the whole mass of people. This is of particular importance with regard to leaders at all levels, especially decisionmakers in economic development units. If they do not have a high awareness of the environment, they may give direction from a psychology that is eager for quick success and instant benefit, with the result that there will be an "eating of food that ancestors provided and creating evil for posterity" in the use of environmental resources. Not only will the environment be sacrificed, but a situation of the more hurry the less speed will be created in developing the economy. Certainly, in the new situation in which policy-making is to be made gradually more democratic and more scientific, efforts to raise the broad masses of the people's environmental awareness is fundamental.

Improvement of environmental awareness requires not just reliance on direct apprehension or indirect experience with environmental problems, but also reliance on the accumulation of scientific knowledge about the environment. This requires energetic publicity and education about environmental protection. China's environmental education has three major characteristics including scientific characteristics that includes knowledge from many different disciplines, applicability to all the people whereby everyone is subjected to education, and a whole journey that runs through everyone's whole life. Furthermore, in addition to education in school, attention should also be given to the use of various publicity techniques to educate society as a whole about the environment. The main ways of doing this can be running an environmental publicity month and a world environment day campaign, having environmental protection exhibitions and environmental protection knowledge tests and competitions, as well as the use of newspapers, magazines, pictures, movie films, and television and radio broadcasts.

To summarize the above, thanks to the high degree of attention that the Chinese Government accords environmental protection, particularly making it a fundamental national policy, we have full confidence in being able to coordinate needs in socioeconomic development with the natural environment's ability to support it to build a benign cycle between the two that makes the good earth of the motherland thrive and prosper.

9432/6091

Expert Urges Efforts To Control Pollution

40101007 Beijing XINHUA in English 5 Jun 88

[Text] Beijing, June 5 (XINHUA) -- A leading Chinese environmental expert Li Kang has called for national attention to environmental pollution and ecological imbalance which "has become serious enough to directly hamper China's economic construction."

In an interview with XINHUA on the world environment day today, the professor with the Chinese Academy of Environmental Science compared the seriousness of pollution in present-day China to that in developed countries in the 1960's.

"It's high time to bring it under control," said Li, 57, also a research fellow with the China Environmental Strategy Research Center.

According to him, China now discharges 7,000 billion cubic meters of waste gas, 33 billion tons of waste water, and more than 600 million tons of solid wastes each year.

Most of the polluted areas are in industrially-developed Southeast China, he noted.

While soil erosion resulting from forest and grassland damage is affecting one-sixth of the Chinese territories, animal and plant resources are threatened and there are more acid rains, the professor said.

To solve the problem, he said, a theoretical breakthrough has to be made so as to find out ways to coordinate the increase of population, social materials, and natural resources.

He believed that it is necessary to include environmental protection in the development plans of the state, different regions, departments and enterprises.

"An appropriate proportion of national income should be invested in environmental improvement," he said.

It is estimated that if an annual average of 1.5 percent of the national income is used as environmental protection investment, China will be able to maintain the quality of its environment in 1990 at the level of 1980.

On China's environmental protection strategy, Li Kang said that pollution should be reduced to the minimum through policy readjustment, rational distribution of the economic enterprises, a comprehensive exploitation of natural resources and the adoption of new technology.

Calling for strict supervision and management of polluted areas, he suggested that restrictions be imposed on the amount of waste discharge.

Permits should be required for pollutant discharge and fees collected for their treatment, he said.

He called for more and detailed decrees governing environmental issues, believing that the existing regulations are too general. "When conditions permit, we should establish environmental courts," he said.

/12223

Current Status of CAE, Mechanical Structure Analysis

40080158a Beijing JIXIE GONGYE ZIDONGHUA [MACHINE-BUILDING INDUSTRY AUTOMATION] in Chinese No 1, Jan-Mar 88 pp 2-11

[Article by Li Shilian [2621 1597 1670]: "One Conception of the Current Situation Regarding CAE and Its Domestic Growth--the Part for Mechanical Structural Analytic Methods"]

[Excerpts] Summing up what has just been said, we can see that people abroad have structure analysis software systems that are quite powerful, and here in China, too, we have made a good foundation in aspects of programs for finite analysis. If we are to rapidly and effectively develop structural analysis software that is suited to the mechanical industry in China, while importing and assimilating advanced foreign software, we should better develop one or two wide-ranging general purpose analysis program systems and various specialized high performance software in accordance with the characteristics of the types of different mechanical products. Those two kinds of software can joint to solve structural analysis and optimal design problems in the mechanical industry.

To clarify the current software systems already developed abroad and to determine the demands made on structural analysis by 24 mechanical product CAD systems developed in China during the 7th 5-Year Plan, we have made a special comparison of the various functions of the 15 structural analysis program systems currently popular internationally (including finite element and boundary element analysis systems). We have also made a preliminary analysis and forecast regarding the demands on the structural analysis functions in regard to the design of the 24 mechanical products. We have listed all specifications for comparison and analysis, and have sought the demand for the basic trends in developing CAE systems suited to China's mechanical industry. This material is shown in Figures 6 and 7. [Figures 6 and 7 on following pages.]

We can see from Figure 6 that the functions of the TITUS, NASTRAN, SAP7, ANSYS, and DIAL system are quite complete and can cover the majority of

Figure 6. A Comparison of the Characteristics and Functions of 15 Finite Element and Boundary Element Systems

System Name: / Item of Comparison:	ADINA	ANSYS	APPLE-SAP	ASAS	ASKA	BEASY	BERSA-FE	DIAL	FESPAC	FLASH2	MARC	MSC/NASTRAN	PAFEC 75	SAP7	TITUS (SYSTUS)
Analytical Functions:															
static	0	0	0	0	0	0	0	0	0	0	0	0	0	0	0
dynamic, transition	0	0	0	X	0	X	0	0	X	X	0	0	0	0	0
call and response	0	0	0	0	0	X	0	0	X	X	0	0	0	0	0
buckling stability	0	0	X	X	0	X	X	0	X	0	0	0	0	0	0
response after buckling	0	0	X	X	X	X	X	0	X	X	0	0	X	0	0
fracture mechanics	0	0	X	0	0	X	0	0	X	X	0	X	0	X	0
heat conduction	0	0	0	0	0	0	0	0	X	X	0	0	0	X	0
special features	F	X	E,S	X	L	X	X	X	X	X	X	L	L	X	E,L
Element Types:															
bar (truss), beam	0	0	0	0	0	X	0	0	0	0	0	0	0	0	0
2-dimen. solids	0	0	0	0	0	0	0	0	0	0	0	0	0	0	0
3-dimen. solids	0	0	0	0	0	0	0	0	X	X	0	0	0	0	0
axial-symmetric solids	0	0	0	0	0	0	0	0	0	0	0	0	0	0	0
flat-bends	0	0	0	0	0	0	0	0	0	0	0	0	0	0	0
shells	0	0	0	0	0	X	0	0	X	0	0	0	0	0	0
boundary elements	X	X	0	X	X	0	X	0	X	X	X	X	0	0	0
fluid elements	0	X	X	0	0	X	X	0	X	X	0	0	0	X	0
Material Characteristics:															
linear elasticity, isotropic	0	0	0	0	0	0	0	0	0	0	0	0	0	0	0
linear elasticity, non-isotropic	0	0	0	0	0	X	0	0	X	0	0	0	0	0	0
non-linear elasticity	0	0	X	X	0	X	0	0	0	0	0	0	0	0	0
viscoelasticity, creep	0	0	X	X	0	X	0	0	X	X	0	0	0	X	0
plasticity	0	0	X	X	0	0	0	0	X	X	0	0	0	0	0
large deformation	0	X	X	X	0	X	X	0	X	X	0	X	X	X	0
soil mechanics materials	0	X	X	X	0	X	0	X	X	0	0	X	X	0	X

[Figure 6 continued on following page]

[Figure 6 continued]

Pre- and Post-Processing Functions:															
automatic net generation	X	0	0	0	0	X	0	0	X	0	0	0	0	0	0
self-coding node numbers	X	0	X	X	0	X	0	0	X	0	X	0	0	0	0
plotting routines	0	0	0	0	0	X	0	0	0	0	0	0	0	0	0
graphics	0	0	X	X	0	X	0	0	0	0	0	0	0	0	0
minor structure method	0	0	X	0	0	0	0	0	X	X	0	0	0	0	0

where: 0 indicates usable; X = unusable; F = various field problems;
S = soil problems; L = linked fluid and structure problems;
E = earthquake

Figure 7. A Demand Forecast for the Structural Analysis Functions of 24 CAD Systems That Are Major Products of the Chinese Machine Industry

Item of Comparison: / Category of Mechanical Product:	Vehicles	Small-to-Medium-Efficiency Asynchronous Machines	Large-Scale Generating Equipment and Systems	Industrial Steam Turbines	Large-Scale Power Transformers	Drill-Type Combination Lathes	Boring-Mill NC Processing Center	Multiple Knife Tools	Presses	Small-to-Medium-Efficiency Internal Combustion Engines	Wheeled Tractors and Cultivators	Bridge Cranes	Wheeled Loaders	Basic Parts for Heavy Machinery	Turbine Compressor CAD/CAM Integration	Ventilation Refrigeration	Petroleum Auger Mining Equipment and Parts	General Purpose Roller Bearings	Special Bearings	Manufacture of Export Instrumentation	Analytical Instrumentation	Optical Instrumentation	Hydraulic Components and Systems	Chain-Drive Components and Systems	Machinery Plant Design
Analytical Functions:																									
static	0	0	0	0	0	0	0	0	0	0	0	0	0	0	0	0	0	0	0	(0)	(0)	(0)	0	0	0
dynamic, transition	0	0	0	0	0	0	0	0	0	0	0	0	0	0	0	0	0	0	0	(0)			0	0	0
call and response	0	0	0	0	0	0	0		0	0	0	0	0	0	0	0		0	0	(0)			0	0	0
buckling stability	0		0						0	0		0		0			0								0
response after buckling												0					0							0	0
fracture mechanics	0		0	0				0						0			0		0						
heat conduction	0	0	0	0	0	0	0	0	0	0	0	0	0	0	0	0	0	0	0	(0)	(0)	(0)			0
special : field	0	OM	OM	OT	OM	OT	OT	OT		OT	OT			OT	OT			OT	OT			L			OT
features : fluids	0			0							0				0	0	0	0			(0)		0		
Element Types:																									
bar (truss), beam	0	0		0	0	0	0	0	0	0	0	0	0	0	0	0	0	0	0	(0)	0	0	0	0	0
2-dimen. solids	0	0	0	0	0	0	0	0	0	0	0	0	0	0	0	0	0	0	0	(0)	(0)	(0)	0	0	0
3-dimen. solids	0	0	0	0	0	0	0	0	0	0	0	0	0	0	0	0	0	0	0	(0)	(0)	(0)	0	0	0
axial-symmetric solids	0	0	0	0		0	0	0	0	0	0	0	0	0	0	0	0	0	0		(0)	(0)	0	0	
flat-bends	0		0	0	0	0	0		0	0	0	0	0	0	0	0	0	0	0	(0)		(0)		0	0
shells	0	0	0	0	0	0	0		0	0			0	0	0	0				(0)					0
boundary elements	0		0	0				0	0	0				0	0										
fluid elements	0		0	0	0	0	0		0	0				0	0	0		0	0				0		
Material Characteristics:																									
linear elasticity, isotropic	0	0	0	0	0	0	0	0	0	0	0	0	0	0	0	0	0	0	0	(0)	(0)	(0)	0	0	0
linear elasticity, non-isotropic								0	0		0	0	0	0				0	0						0
non-linear elasticity								0	0		0			0	0			0	0						
viscoelastic creep						0	0		0		0			0			0	0	0						0
plasticity						0	0	0	0																
large deformation									0																
soil mechanics materials											0														0
Pre- and Post-Processing Functions:																									
automatic net generation	0	0	0	0	0	0	0	0	0	0	0	0	0	0	0	0	0	0	0	(0)	(0)	(0)	0	0	0
self-coding node numbers	0	0	0	0	0	0	0	0	0	0	0	0	0	0	0	0	0	0	0	(0)	(0)	(0)	0	0	0
plotting routines	0	0	0	0	0	0	0	0	0	0	0	0	0	0	0	0	0	0	0	(0)	(0)	(0)	0	0	0
graphics	0	0	0	0	0	0	0	0	0	0	0	0	0	0	0	0	0	0	0	(0)	(0)	(0)	0	0	0
minor structure method	0	0	0	0	0	0	0	0	0	0	0	0	0	0	0	0	0	0	0						0
optimal design	0	0	0	0	0	0	0	0	0	0	0	0	0	0	0	0	0	0	0	(0)	(0)	(0)	0	0	0

where: 0 indicates necessary; (0) = can consider implementing; T = temperature field; M = magnetic field; L = lens system computers

the demands from structural analysis. We can see from Figure 7 that there are distinct gaps in the 24 products of China's mechanical industry regarding the requirements of analytical functions and element types, but that they are rather thoroughgoing for the requirements for pre- and post-setting and processing and for optimal design. At present, we in China have developed some finite element analysis programs for the areas of static, dynamic, and temperature stress on internal combustion engine components and lathe components, and we have done preliminary research in optimal design of internal combustion engines, as well as for pre- and post-setting and processing of structural analysis. From now on, we should adopt the strong points of advanced foreign software in accordance with what we already have, and in a planned and organized way develop structural analysis software systems that conform to the demands of China's mechanical industry, gradually forming as we do a unified CAD/CAM/CAE system.

A preliminary conception of the basic method for developing a CAE system for China's mechanical industry would be as follows:

1. We should establish two levels of CAE systems, high and low in accordance with the power of the CPU. The low level would be for general purpose machines, can satisfy a large number of general requirements, and would be for 16-bit and 32-bit microcomputers (as for example, the IBM XT, IBM AT, GW-286, and BF-386). SAP5 has long been used in China, and recently SAP6 with more functions has been transplanted to microcomputer, which established SAP6 as the basis for the standard for a general system. The high level system would be for very high performance computers and is suitable for use in superminis (such as the VAX 8500) and medium size computers (such as the IBM 4381) or high level workstations (such as the Apollo DN4000). Some units in China already have the original ADINA and NASTRAN programs or are currently importing the SYSTUS and ANSYS systems, and we could consider forming a domestic high level CAE system from those systems.

2. We would arrange for relevant mechanical industries to develop specialized CAE software with the standard systems just described in mind. For example, plastics molding, electromechanics, and fluid mechanics could develop standardized high efficiency specialized CAE software.

3. To better disseminate and apply these systems we should pay attention to developing pre- and post-processing software that is suitable for China's national situation, and that therefore has the features of Chinese text handling and ease of learning and using.

12586/09599

New Version of AI Language, f-Prolog, Described

40080158b Shenyang XIAOXING WEIXING JISUANJI XITONG [MINI-MICRO SYSTEMS] in Chinese Vol 9 No 5, May 88 pp 26-31

[Article by Liu Dongbo [0491 2639 3134] and Li Deyi [2621 1795 3015], both of PLA General Staff, Institute No 61]: "The Fuzzy Prolog Language and Expert Systems"; word in slantlines published in English in original]

[Excerpts] Abstract: The Fuzzy Prolog language has opened up channels in the research of expert systems. This paper seeks to describe a new version of the Fuzzy Prolog language--f-Prolog--intending to explain its fundamental grammar, as well as its differences with traditional Prolog. Furthermore, it pays special attention to knowledge representations and uncertain inferences, and points out that because traditional modes of knowledge representation and inference methods lack a necessary fuzzy logic methodology, they therefore exclude large quantities of fuzzy information and empirical knowledge. By use of examples, this paper also shows that f-Prolog is not only an excellent tool for knowledge representation it is also quite suited as an inference engine for expert systems.

I. Preface

As a logical program design language, traditional Prolog has provided an excellent development tool for expert systems rooted in regular inference. It has not only been successfully employed as a predicate calculus, notably as Horn's clausal logic, but has also been used because of its unique witty style, and has consequently been rather favored.

In recent years, research in the field of expert systems has achieved exciting results, and expert systems can represent and apply the actual knowledge of experts in certain fields to solve problems. For example, through the combined efforts of human experts and system developers, there are expert system that can now diagnose symptoms and do prospecting in mines, as well as analyze chemical structural formulas

(MYCIN, PROSPECTOR, and DENDRAL). Some of these can even perform better than human experts.

However, when it comes to simulating the logical thinking of human experts, this is done at present through binary logic as implemented based on the regular forms of mathematical logic. In principle, they cannot reproduce the complex random conceptualization process of "from continual to discrete" as a dynamic determinative model that is a tool of logic. That is to say, in logic formalization, that which is reproduced is merely the static state of thinking, not the dynamic process, and what is fixed is merely the results of thinking, not an unfolding of the dialectic development process.[1,2]

With the continuing intensification of the scientific study of artificial intelligence and recognition, and especially the deepening knowledge of the contradictions between "complex large systems" and "accuracy," now that fuzziness has undergone the rigors of contemporary mathematical theory, it has become more and more respected by developers of expert systems. They realize that describing "complex large systems" with binary logic, not to mention simulating the thinking process of experts, is entirely insufficient. Where there is no clear distinction between true and false, people will use their capacities for flexibly processing fuzzy phenomena, and will undertake an integral parallel conceptualization that will consequently be capable of creative thinking that is inclusive, abstract, and intuitive.[3]

Some expert systems have incorporated an approximation inference method based on probability,[4,5] but without the necessary fuzzy logic methodology; the input and processing of a lot of fuzzy information and experience has been excluded; and, in our opinion, fuzziness is a fundamental characteristic of human thinking. To simulate the thinking of experts in an expert system of one's own urgently requires a development tool that is based upon fuzzy mathematics and fuzzy logic.

To confront this situation, we have accepted the theories of L.A. Zadeh,[6] M.H. Van Emden, and R.A. Kowalski[7,8,9] to establish a set of fuzzy inference theories based on a finite set of Horn's clause rules,[10,11,12] and have also similarly developed an original fuzzy Prolog language--f-Prolog.[12]

The f-Prolog system is not only capable of fuzzy inferences, but also maintains the features of pattern matching and backtracking of the traditional Prolog. As far as program design methods and style are concerned, they too are very similar to those of traditional Prolog, and they are easier to use. With the support of f-Prolog, it is expected that expert systems will make new advances.

II. An Introduction to f-Prolog

The program f-Prolog solves problems in a manner similar to that of traditional Prolog, and that approach is usually made up of three primary portions:

1. States facts (or assertions) explaining relations between the objects concerned;

2. defines some rules for relations between objects;

3. and proposes problems about particular relations (or goals) between objects.

The f-Prolog language employs three kinds of statements to delineate the three portions just described:

1. f-facts A:-[f]-, representing the fact that A has a degree f of truth confidence, or that the truth value of A is f.

2. f-rules A:-[f]- $B_1,B_2,\ldots,B_n$, which indicates that the implicit strength of conclusion A for the condition $B_1 \hat{} B_2 \hat{} \ldots \hat{} B_n$ is f, that is, if the truth value of B_i is $tv(B_i)$, where $i=1,2,\ldots,n$, then the truth value of the condition is $t=\min\{tv(B_i)|i=1,2,\ldots,n\}$ (see L.A. Zadeh[6]), and furthermore, the truth value of the conclusion is $tv(A)=f \times t$ (see reference 11).

3. f-goals ?-[f]-$B_1,B_2,\ldots B_n$, (f is a constant) which means "when the value in brackets is f, will $B_1,B_2,\ldots B_n$ uniformly satisfy it?", or, ?-[F]-$B_1,B_2,\ldots,B_n$, (F is a variable) which means that you want to solve for the degree of truth confidence for $B_1 \hat{} B_2 \hat{} \ldots \hat{} B_n$.

In form, the statements of f-Prolog are identical with those of traditional Prolog, but the introduction of the degree of inference f, as well as the expansion of the truth value concept from {0,1} to [0,1], cause its capacities to describe and infer to exceed those of traditional Prolog.[12] One thing that is well worth mentioning is that the degree of inference may be not only a constant or variable, but also a function. In that instance, the knowledge base must provide the necessary subordinate function (we cannot help but see this as a fourth type of statement in f-Prolog: f-function), and will use the internal predicate /function/ to define it. Thus, the research achievements of the fuzzy set theory can be conveniently used within the f-Prolog language.

III. Knowledge Representation

A very good mode of knowledge representation is essential to solving complex problems because the process of intellectual activity is a process of obtaining and using knowledge. Knowledge representations in

expert systems are simply a study of how to use the most appropriate form to organize knowledge and to enable it to be most useful for solving problems. Generally speaking, how to represent knowledge most appropriately is closely related to the problem to be solved and to its methodology.

1. Modes of traditional knowledge representation

Widely used modes of knowledge representation at present include: the logical representation mode, the semantic network representation mode, the generative rule representation mode, and the frame representation mode.

The logical representation mode was first used as one mode of knowledge representation in the field of artificial intelligence, and primarily describes some facts and rules through the propositional and predicate calculi of mathematical logic. The chief characteristic of logical representation is that its deductive result maintains accuracy within a certain range, while to date the other knowledge representations have yet to attain that goal. Another reason that modes of representation based on logic have been widely used in artificial intelligence is that the method by which new facts can be inferred from known facts can be mechanically constituted. The inductive principle of Robinson[13] provides the theoretical basis for this.

The semantic network acts as a kind of knowledge representation technology and has been widely applied. It originated as an explicit psychological model for human associative intelligence. Generally speaking, a semantic network is a directed graph composed of nodes that are represented entities and concepts, and solitary lines indicating relations between nodes. Because relations can be of many different kinds, this means that the representative capacity of semantic networks is quite extensive. The natural language processing system of Simmons (1973) and the prospecting expert system PROSPECTOR[5] are founded upon this kind of representation.

The generative rule representation mode is what is most often used in expert systems. It transforms expert knowledge into line by line of generative rules, the first component of which describes the status, while the last describes the action. Because there is independence among the various forms generated, establishing a system with this mode allows revision and expansion to be quite convenient. The famous medical consultation expert system MYCIN[4] uses this mode of knowledge representation.

The frame mode of expression was proposed during Minsky's 1974 research into the field of computer vision as an inspiration from recognizing and understanding the problem of visual images. The frame is a data structure that describes certain patterns. It consists of a group of slots, and a frame can have any finite number of slots, a slot can have

any finite number of sides, and a side can have any finite number of values. The frame, slot, and side can describe various kinds of information, while the value of the side can also be another frame. The proposal of this mode of knowledge representation has great significance, but because it has been only recently developed it is still in an immature stage...

IV. The Inference Engine

An inference engine in an expert system is a group of routines used to control and adjust the entire system. Basing itself upon currently input information (data or graphics), it uses knowledge in the knowledge base to solve the current problem in accordance with particular policies.

Because the expert system emulates the progress of human experts, when designing the inference engine, its inferential process should be made to be as similar to that of the inferential process of the expert as possible.

1. Control principles

Forward inference, backward inference, and bilateral inference are commonly used in expert systems.

Forward inference is also called event-driven inference. It begins from the original data and reaches its conclusion in accordance with particular principles and using the knowledge of experts from a knowledge base. There are two unavoidable problems with this inferential process: one, it is extremely wasteful of time; and two, its inference is quite blind. Naturally, these two problems are related.

Backward inference is also called goal-driven inference. It first proposes its conclusion (hypothesis), after which it seeks proof by which to support this conclusion. The principle advantage of this deductive inference is that the inference has a goal, but it also has some difficulties. For example, when in the decisionmaking process many tentative hypotheses (or goals) must be considered, or when the attempt obtains proof that is related to these hypotheses, this creates difficulties for the inference.

When actually establishing expert systems, most people use the backward inference method, but theoretically, forward inference and backward inference are equivalent, that is, they will generate equally correct conclusions. Naturally, if different controlling principles are used, the paths by which conclusions are reached will be different.

For many problems, forward and backward inference may both be used independently. Sometimes the two may be combined for inference, what we

called the "bilateral inference." This trade-off inference method first helps the system propose a hypothesis in accordance with original data in the data base and through forward inference, and then it uses backward inference to further seek evidence supporting the hypothesis.

2. Imprecise inference

We know that with precise inferences, knowledge of a field becomes represented as necessary causal relations and logically inferred relations, and that the inferred conclusions can be either affirmative or negative, but must be one or the other.

But in actual practice, people actually use imprecise inferences, and since the expert system is modeled on the working of the human expert, this aspect must be adequately respected.

Among imprecise inferences, there are different degrees of affirmation and denial regarding evidence. The relation between the first and last clauses of a rule are "loose," that is, there is attenuation of the strength of the causal relations and logical inferences. We must then label the degree of proof affirmation as the "degree of truth confidence," while calling the attenuation factor for causal relations and logical inferences "degree of rule." Inaccurate inference is an integration of the degrees of truth confidence and rule for a series in the knowledge base, and different imprecise inferences can be reached because of different distortions of the method of integration.

At present, among popular imprecise inference methods are the believability method of the MYCIN system[4] and the Bayes method of the PROSPECTOR system.[5] But as far as the reality behind the problem is concerned, those systems can only delineate the probability characteristic of a problem, and they lack a background in fuzzy logic methodology when it comes to the essential characteristic of human cognition--fuzziness. This is because randomness and fuzziness (possibility) are two indeterminatives of different natures.[14]

V. Conclusions

Knowledge representations and imprecise inferences are not only very important in expert systems, but have an extremely important position as well within the entire knowledge process even throughout the whole of artificial intelligence.

In the process of developing expert systems, we have thoroughly realized that a simple search for precision will be certain to exclude a large amount of fuzzy information and empirical knowledge. This fact is in contradiction with the simulation of human expert thinking by expert systems. The achievement of f-Prolog will unquestionably stimulate the research and development of expert systems.

References

1. Miao Dongsheng [5379 2639 0581]. A Primer for Fuzzy Study. People's University Publishing, 1987.

2. Li Xiaoming [2621 2556 2494]. Fuzziness: The Mystery of Human Intelligence. People's Publishing, 1985.

3. He Zhongxiong [6320 0112 7160]. Fuzzy Mathematics and Its Applications. Tianjin Science and Technology Publishing, 1982.

4. Shortliffe, E. Computer Based Medical Consultations: MYCIN. New York: American Elsevier, 1976.

5. Duda, R.O., et al. "Development of the Prospector Consultation System for Mineral Exploration." Annual Report SRI Projects 5821 and 6415. Artificial Intelligence Center, SRI International, Menlo Park, California, 1977.

6. Zadeh, L.A. "Fuzzy Sets." Inform. and Control 8(1965): 338-353.

7. Van Emden, M.H. "Quantitative Deduction and Its Fixpoint Theory." J. of Logic Programming, 1(1986): 37-53.

8. Van Emden, M.H. and R.A. Kowalski, "The Semantics of Logic as a Programming Language." J. ACM, 23(1976): 733-742.

9. Kowalski, R.A. "Predicate Logic as Programming Language." Proc. IFIP74, North Holland, Amsterdam, 1974, 569-574.

10. Liu Dongbo and Li Deyi. "Solution of Fuzzy Problems Using the f-Horn Clauses." Conference Papers of the First National Conference on Automatic Inference. 1987.

11. Liu Dongbo and Li Deyi. "Quantitative Development of Logical Inference Theories." Papers of the Third National Research Conference on Logic Program Design and Artificial Intelligence Languages. 1987.

12. Liu Dongbo. "A New Fuzzy Inference Theory and the f-Prolog System." Masters thesis. 1987.

13. Robinson, J.A. "A Machine-Oriented Logic Based on the Resolution Principle." J. ACM, 12.1(Jan. 1965): 23-41.

14. Zadeh, L.A. "Fuzzy Sets as a Basis for a Theory of Possibility." FSS 1(1978): 3-28.

12586/09599

PHOTOLUMINESCENCE DIAGNOSIS OF GaAs/GaAlAs MULTIPLE QUANTUM WELLS

40090125a Beijing WULI XUEBAO [ACTA PHYSICA SINICA] in Chinese Vol 37 No 6, Jun 88 pp 906-915

[English abstract of article by Jia Weiyi [6328 1919 5030], et al., of the Institute of Physics, Chinese Academy of Sciences]

[Text] The photoluminescence technique is used to diagnose the quality of quantum wells. The influences on the fluorescence spectra of quantum wells due to thickness fluctuations of the quantum wells, fluctuation of the aluminum content, various defects and unintentional impurities are discussed. In addition, the possible reasons causing the degradation of the quantum wells are deduced from the photoluminescence spectra. To some extent the diagnosis can provide certain basic information for improving molecular beam epitaxy technology.

9717

RESEARCH ON ABLATION OF METAL BY UV LASER

40090127a Shanghai YINGYONG JIGUANG [APPLIED LASER] in Chinese Vol 8 No 3, Jun 88 pp 97-100

[English abstract of article by Li Shixin [2621 1102 2450], et al., of Shanghai Institute of Optics and Fine Mechanics]

[Text] The ablation processes of metal film by UV excimer lasers are analyzed theoretically in this paper. The effects of the thermodynamic characteristics of the materials on the ablation processes are also investigated. The linear relationship between the ablation rate and laser energy density at the metal surface is in good agreement with that of the experiments. For Cu film, when the laser energy density is about 25 J/cm^2, the ablation rate can be as high as 0.8 micrometer per pulse.

9717

INVESTIGATION OF STIMULATED RAMAN SCATTERING IN Pb VAPOR

40090127b Shanghai YINGYONG JIGUANG [APPLIED LASER] in Chinese Vol 8 No 3, Jun 88 pp 101-104

[English abstract of article by Qi Jianping [4359 1696 1627], et al., of the Institute of Crystal Materials, Shandong University; Lou Qihong [2869 4388 3163], et al., of Shanghai Institute of Optics and Fine Mechanics, Chinese Academy of Sciences]

[Text] The parametric dependence of the output energies and efficiency for the Raman conversion of XeCl excimer laser radiation in Pb vapor was studied. Pulses at Raman-shifted wavelength, with 120 mJ energy and 2 MW peak power, were obtained. The effects of the buffer gas on the stimulated Raman scattering in Pb vapor are analyzed theoretically. The theoretical results show that the effects consist of the collision effects between buffer gas atoms and Pb atoms and the absorption effects of the buffer gas. The calculated results are in agreement with the experimental ones.

9717

STUDY OF CAVITY LENGTH DETUNING EFFECT ON SYNCHRONOUSLY PUMPED MODE-LOCKED CW DYE LASER

40090127c Shanghai YINGYONG JIGUANG [APPLIED LASER] in Chinese Vol 8 No 3, Jun 88 pp 107-110

[English abstract of article by Yin Yiyan [0603 5030 6056], et al., of Nanjing Institute of Technology]

[Text] The effect of cavity length detuning on the output parameters of the synchronously pumped mode-locked CW dye laser has been studied in this paper. The experimental results, including the relationship among the pulse width, average output power of the dye laser and the cavity length detuning, and the relationship among the pulse width, line width and pumping power, are given with reasonable theoretical explanations.

9717

NOVEL TUNABLE CRYSTAL CANDIDATE Cr^{3+} DOPED BERYLLIUM HEXA-ALUMINATE (BHA:Cr^{3+})

40090126a Shanghai ZHONGGUO JIGUANG [CHINESE JOURNAL OF LASERS] in Chinese
Vol 15 No 7, 20 Jul 88 pp 403-407

[English abstract of article by Ma Xiaoshan [7456 4562 1472], et al., of Shanghai Institute of Optics and Fine Mechanics, Chinese Academy of Sciences]

[Text] Beryllium hexa-aluminate crystal doped with chromium (BHA:Cr^{3+}) has been grown for the first time. The absorption and fluorescence spectra of BHA:Cr^{3+} have been measured, and the vibronic side band of the fluorescence spectra ranges from 700 to 1000 nm.

9717

ANALYSIS OF STABILITY OF MÖLLENSTEDT BIPRISM

40090126b Shanghai ZHONGGUO JIGUANG [CHINESE JOURNAL OF LASERS] in Chinese
Vol 15 No 7, 20 Jul 88 pp 408-411, 430

[English abstract of article by Fu Shufen [0265 3219 5358] of Shanghai Institute of Optics and Fine Mechanics, Chinese Academy of Sciences]

[Text] Regarding electrons as waves, the author obtained an expression for phase changes produced by a Möllenstedt biprism. The mechanical stability effect of the biprism on the interference field was analyzed based on the expression. A scheme for a stable biprism is given and the results of electron interference and electron holography are presented with this biprism as an electron beam splitter.

9717

STUDY OF $Y_3Ga_5O_{12}:Cr^{3+}$ LASER CRYSTAL BY MEANS OF MS-Xα METHOD

40090126c Shanghai ZHONGGUO JIGUANG [CHINESE JOURNAL OF LASERS] in Chinese
Vol 15 No 7, 20 Jul 88 pp 412-416

[English abstract of article by Wen Genwang [2429 2704 2489], et al., of the Department of Physics, Hunan Normal University, Changsha; Liu Songhao [0491 7313 6275] of the Institute of Quantum Electronics, South China Normal University, Guangzhou]

[Text] This paper reports the calculated results of a $(CrO_6)^{9-}$ transition metal cluster on the D_{3d} symmetry site by means of the unrestricted spin MS-Xα method. It presents the single electronic eigenvalues and wave functions, discusses the electronic structure of $Y_3Ga_5O_{12}:Cr^{3+}$ laser crystals and calculates the $10D_q$ crystal field parameter and the energy splitting due to the low symmetry distortion of the lattice site by the Slater transition state concept. The calculated results are in good agreement with the experimental ones.

9717

EFFECTS OF BUFFER GAS ON STIMULATED RAMAN SCATTERING IN Pb VAPOR

40090126d Shanghai ZHONGGUO JIGUANG [CHINESE JOURNAL OF LASERS] in Chinese
Vol 15 No 7, 20 Jul 88 pp 421-424

[English abstract of article by Qi Jianping [4359 1696 1627] of the Institute of Crystal Materials, Shangdong University, Jinan; Lou Qihong [2869 4388 3163], et al., of Shanghai Institute of Optics and Fine Mechanics, Chinese Academy of Sciences]

[Text] Effects of buffer gas on stimulated Raman scattering in Pb vapor are analyzed theoretically. The results show that the effects consist of the collision between the buffer gas atoms and the Pb atoms and the absorption of the buffer gas. The dependence of the Raman conversion efficiency on laser parameters is analyzed. The calculated results are in agreement with those of recent experiments.

9717

EFFECTS OF GAS PRESSURE ON OUTPUT OF TRANSVERSE FLOW CO_2 LASERS

40090126e Shanghai ZHONGGUO JIGUANG [CHINESE JOURNAL OF LASERS] in Chinese
Vol 15 No 7, 20 Jul 88 pp 431-434

[English abstract of article by Wu Zhongxiang [0702 0022 4382], et al., of the Institute of Mechanics, Chinese Academy of Sciences, Beijing]

[Text] Based on the measured parameters of high pressure transverse flow discharge CO_2 lasers and their changing limits, simulated calculations have been made of the theoretical curve of power, efficiency and coupling degrees and their variations with gas pressure. It is indicated that the optimal output of the CO_2 laser can be obtained at a working pressure of ~1 atm, and the CW output will be cut off at ~2 atm.

9717

MEASUREMENT OF DENSITY OF GAP STATES IN AMORPHOUS SEMICONDUCTORS BY INFRARED STIMULATED CURRENTS

40090125b Beijing WULI XUEBAO [ACTA PHYSICA SINICA] in Chinese Vol 37 No 6, Jun 88 pp 916-923

[English abstract of article by Wu Wenhao [0702 2429 6275], et al., of the Institute of Physics, Chinese Academy of Sciences]

[Text] A new method for measuring the density of gap states in amorphous semiconductors by employing a two-beam photoconductivity experiment is reported. In the two-beam experiment, an intensive bandgap pump light is used to create non-equilibrium carriers, and most of these carriers are trapped in the gap states. Then, at a later time t_d, after turning off the pump light, these trapped carriers are re-excited by an infrared probe light. A photoconductivity overshoot, which depends on the delay time and temperature, is observed during the onset of IR excited photoconductivity. The results are discussed using the multiple trapping theory. The distribution of the density of gap states is deduced from the experiment.

9717

GROWTH OF Ag ULTRAMICRO-PARTICLES IN BaO SEMICONDUCTOR FILM

40090125c Beijing WULI XUEBAO [ACTA PHYSICA SINICA] in Chinese Vol 37 No 6, Jun 88 pp 924-930

[English abstract of article by Zhang Xu [1728 2485], et al., of the Department of Radio Electronics, Beijing University]

[Text] The growth of Ag ultramicro-particles in BaO semiconductor film is investigated by a transmissive electron microscope. The fine growth of Ag ultramicro-particles in BaO film is discovered in the samples after proper heat treatment. The authors also contrast the structural differences of single-layer and multilayer Ag + BaO films. The growth properties of Ag ultramicro-particles in Ag + BaO films with different Ag content are also studied. The Ag ultramicro-particles do not form a maze structure in the Ag + BaO film with high Ag content, but form isolated Ag particles. A BaO layer of a few nm thick is present between every two Ag particles.

9717

PROXIMITY EFFECT, MUTUAL DIFFUSION IN a-Ge/Ag LAYERS

40090125e Beijing WULI XUEBAO [ACTA PHYSICA SINICA] in Chinese Vol 37 No 6, Jun 88 pp 950-958

[English abstract of article by Zhang Yuheng [1728 5940 1854], et al., of the Department of Physics, University of Science and Technology of China, Hefei]

[Text] In the present work, the behavior of a-Ge/Ag composite layers is studied. These layers are composed of amorphous Ge film with thickness of 2000 Å and Ag film of different thicknesses. It is found that, when the Ag film thickness decreases, the electrical resistivity of the composite layer at room temperature becomes increasingly smaller than that of the Ag monolayer with the same thickness. The proximity effect at room temperature is shown clearly by the experiment. As the samples are annealed, the authors obtain various $R(T_a-T)$ relationships under different annealing temperatures (T_a) and various levels of dependence of R_{300K} on T_a for layers with different Ag film thicknesses. Based on structural analysis by XRD and composition analysis by EMP, in addition to observation with TEM and SEM, the new phenomena are explained.

9717

CHARACTERIZATION OF MICROSTRUCTURE OF PLASMA SPRAYED SUPERCONDUCTING COATING

40090122c Beijing JINSHU XUEBAO [ACTA METALLURGICA SINICA] in Chinese Vol 24 No 3, Jun 88 pp B220-B223

[English abstract of article by Wen Lishi [5113 4539 2514], et al., of the Institute of Metal Research, Chinese Academy of Sciences]

[Text] A high T_c oxide YBaCuO superconducting coating has been prepared by a plasma spraying method. The structure and phase transformation of the coating during spraying and after the annealing treatment process have been studied by X-ray diffraction, TEM, SEM and DTA techniques. The results show that the as-sprayed coating lost its superconductivity completely at liquid nitrogen temperature and was composed mainly of microcrystalline and amorphous structures. Its superconductivity can be restored by proper annealing at 850-950°C.

9717

CONDUCTIVITY IN DISORDERED LAYER SYSTEM

40090125d Beijing WULI XUEBAO [ACTA PHYSICA SINICA] in Chinese Vol 37 No 6, Jun 88 pp 941-949

[English abstract of article by Jiang Qi [5592 4388], et al., of the Center of Theoretical Physics, Department of Physics, Nanjing University]

[Text] In this paper, the crossover effect of the dimensionality in the disordered layer system is studied by using the post-CPA method for the vertex. The effective dimensionality of the system is determined by the interlayer coupling t. It is shown that Anderson transition will occur at the critical value t_c. The Boltzmann conductivity, dynamic conductivity corresponding to the maximum crossed diagrams, dc conductivity and the localization length near the critical point are calculated.

9717

POSSIBLE HEAVY-FERMION MECHANISM OF SUPERCONDUCTIVITY--ELECTRON-SLAVE BOSON SUPERCONDUCTING MECHANISM

40090125f Beijing WULI XUEBAO [ACTA PHYSICA SINICA] in Chinese Vol 37 No 6, Jun 88 pp 967-973

[English abstract of article by Feng Shiping [7458 0013 1627] of the Department of Physics, Institute of Low Energy Nuclear Physics, Beijing Normal University]

[Text] Using the Anderson lattice, heavy-fermion superconductivity is discussed. Within the long wavelength limit of the Slave boson field, the interaction between the same type of quasiparticles attracts by one-Slave boson exchange and the heavy-fermion superconductivity is induced by the first type of quasiparticles--quasi-f electrons only.

9717

RELATIONSHIP OF SUPERCONDUCTIVITY, STRUCTURE IN $YBa_{2-x}Sr_xCu_3O_{7-\delta}$

40090125g Beijing WULI XUEBAO [ACTA PHYSICA SINICA] in Chinese Vol 37 No 6, Jun 88 pp 1042-1047

[English abstract of article by Zhao Yong [6392 0516], et al., of the Department of Physics, University of Science and Technology of China, Hefei; Sun Dunming [1327 2415 2494], et al., of the Department of Applied Chemistry, University of Science and Technology of China, Hefei]

[Text] The relationship between superconductivity and the phase structure of the $YBa_{2-x}Sr_xCu_3O_{7-\delta}$ system has been studied systematically. It is found that when $0 < x \leq 1.25$, all samples exhibit the 1-2-3 orthorhombic structure of the single phase, but their superconducting critical temperatures do not change monotonously with the Sr content. The superconducting critical temperature shows dramatic dependence on the crystal structure of the samples: with the increase in the difference of a and b, T_c increases monotonously. The mechanism of the effect of the Sr atom on T_c and superconductivity is also discussed.

9717

CHARACTERISTICS OF LOW TEMPERATURE RESISTIVITY OF GRANULAR SUPERCONDUCTOR $Ba_2YCu_3O_{7-\delta}$

40090125h Beijing WULI XUEBAO [ACTA PHYSICA SINICA] in Chinese Vol 37 No 6, Jun 88 pp 1048-1052

[English abstract of article by Yu Daoqi [0827 6670 1142], et al., of the Department of Physics, University of Science and Technology of China, Hefei; Pan Guoqiang [3382 0948 1730], et al., of the Department of Applied Chemistry, University of Science and Technology of China, Hefei]

[Text] The authors have studied the relationship between the low temperature resistance of single phase $Ba_2YCu_3O_{7-\delta}$ and the magnetic field, temperature and measuring current. The results show that the resistance behavior varies with the strength and direction of the field as well as with the measuring current. It is suggested that all results are associated with the granular structure of the sample.

9717

Optimal Design for FDMA Satellite Network

40080119a Shanghai DIANXIN KUAIBAO [TELECOMMUNICATIONS INFORMATION] in Chinese No 2, Feb 88 pp 8-13

[Article by Lin Pinxiang [2651 0756 4382]]

[Excerpts] Rapid growth in satellite communications technologies and their broad range of applications have led to substantial evolution in the composition of satellite networks. Early single networks composed of one type of ground station have become today's mixed networks made up of many types of ground stations ranging from FDMA [frequency division multiple access] satellite networks to TDMA [time division multiple access] satellite networks, satellite TV networks, satellite data networks, and various types of special purpose satellite networks. Thus, the achievement of an optical operational state in all types of satellite networks is a major issue in network design.

I. Satellite Frequency Band Utilization

The bandwidth capacity N_B of a satellite depends on the satellite bandwidth B_P and the radio frequency bandwidth B_{RF} of the signal, so $N_B = B_P/B_{RF}$. Table 1 shows bandwidth utilization for a 36MHz transponder using different forms of modulation.

Table 1. Satellite Frequency Band Utilization (B_P = 36MHz)

Form of modulation	$\Delta M/2\phi$-PSK	$\Delta M/4\phi$-PSK	PCM/4ϕ-PSK	CFM	ACSB
Speed (kb/s)	32	32	64		
Carrier wave bandwidth B_{RF} (MHz)	45	22.5	45	45	4
Bandwidth capacity N_B (channels)	800	1,600	800	800	9,000

It is apparent from Table 1 that there is extreme variation in the degree of bandwidth utilization in a particular satellite using different forms of modulation. For example, a 36MHz transponder can handle 9,000 channels using ACSB [amplitude companded single sideband], but only 800 or 1,600 channels using $\Delta M/2\phi$-PSK [delta modulation/2ϕ phase shift keying), etc.

II. Satellite Power Utilization

Under specific satellite conditions, the power capacity of a satellite N_P is determined primarily by ground station quality factors, signal modulation characteristics, and amount of channel noise. It can be described by the difference between the carrier wave thermal noise ratio $(C/N_0)_t$ the satellite system can provide, and the carrier wave thermal noise density ratio $(C/N_0)_{THM}$ required by each carrier wave. Thus:

$$N_p = \log^{-1}\{[(C/N_0)_T - (C/N_0)_{THM}]/10\}$$

$(C/N_0)_T$ and $(C/N_0)_{THM}$ are the satellite and ground station performance parameter and channel noise function. Channel noise varies with satellite transponder compensation. Under optimal conditions, channel noise is at a minimum or the noise/power ratio is at a maximum and satellite power is used fully.

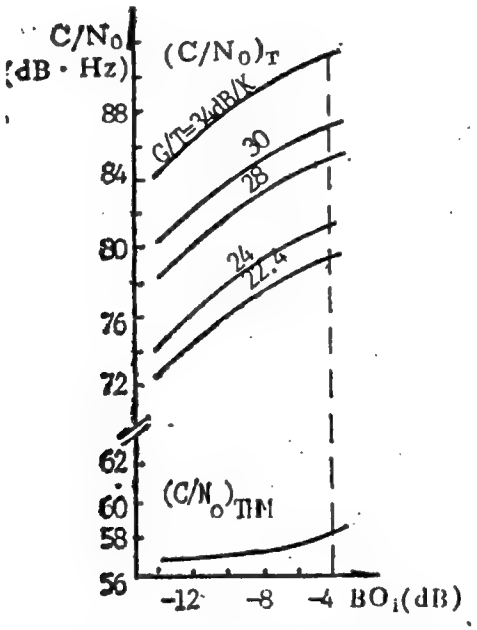

Figure 1. Curve of the Relationship Between C/N_0 and BO_i for $\Delta M/2\phi$-PSK Modulation

Figures 1 and 2 show the curves of the relationship of $(C/N_0)_T$ and $(C/N_0)_{THM}$ with transponder input compensation under different ground station conditions for the same satellite when using $\Delta M/2\phi$-PSK, respectively. Figures 3 and 4 show the curves of the relationships between satellite power capacity N_P and input compensation BO_i, respectively. It is apparent from Figures 3 and 4 that:

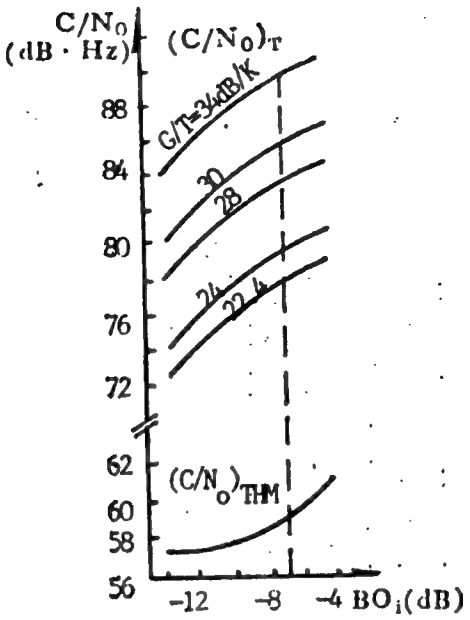

Figure 2. Curve of the Relationship Between C/N_0 and Bo_i for $\Delta M/4\phi$-PSK

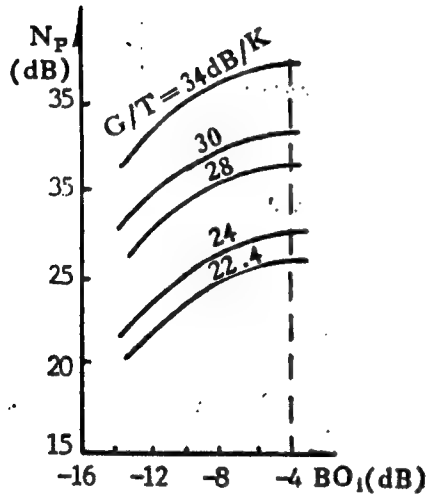

Figure 3. Curve of the Relationship Between N_P and BO_i for $\Delta M/2\phi$-PSK Modulation

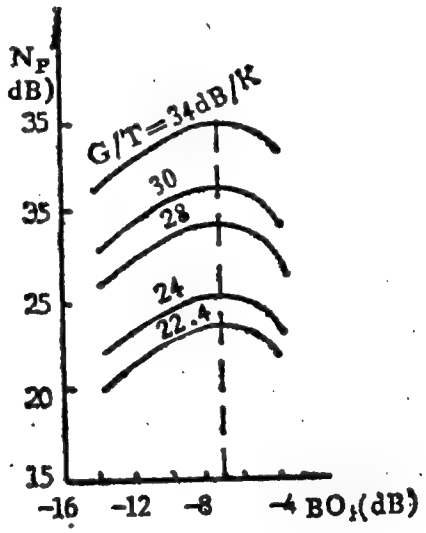

Figure 4. Curve of the Relationship Between N_P and BO_i for $\Delta M/4\phi$-PSK Modulation

1. When the same type of ground station uses the same form of modulation but different compensation, there are differences in satellite power utilization. There is one optimal value. In this example, the optimal value appears when BO_i = -4dB with $\Delta M/2\phi$-PSK and when BO_i = -7dB with $\Delta M/4\phi$-PSK.

2. When different types of ground stations use the same form of modulation, there also will be differences in the utilization of power from a particular satellite. The larger the ground station G/T value, the better the power utilization. As shown in Figure 4, for example, G/T = 34dB compared with 30dB, so the former utilizes about 4dB more.

3. When ground stations with identical G/T values employ different forms of modulation, there also will be differences in the degree of power utilization for a particular satellite. Comparing Figures 3 and 4, it is apparent that $\Delta M/2\phi$-PSK is capable of more effective utilization of satellite power than $\Delta M/4\phi$-PSK (about 2dB more).

III. Optimal Design of Satellite Networks

There are two basic types of satellite networks. One is a single ground station which forms a single network, and the other is a mixed network composed of many types of ground stations. Methods for optimal network design will be described below in terms of capacity.

1. A single satellite network using the same type of ground station

A single satellite network is the simplest and most basic network. Because all ground stations in this type of network have identical G/T values, network capacity N_I can be derived by comparing bandwidth capacity N_B with power capacity N_P. Thus, when $N_B > N_P$, $N_I = N_P$; when $N_B = N_P$, $N_I = N_B = N_P$; when $N_B < N_P$, $N_I = N_B$. Table 2 provides some examples of capacity.

Table 2. Examples of the Capacity of Single Satellite Networks (Satellite EIRP = 28dBW)

Ground $(G/T)_E$ (dB/K)	$\Delta M/2\phi$-PSK			$\Delta M/4\phi$-PSK		
	N_B Ground station	N_P Number of channels	N_I Number of channels	N_B Ground station	N_P Number of channels	N_I Number of channels
34	800	5223	800	1600	2694	1600
31.28	900	2805	800	1690	1600	1600
30	800	2103	800	1600	1199	1199
28	800	1330	800	1600	769	760
25.8	800	800	800	1600	460	460
24	800	530	530	1600	304	304
22.4	800	367	367	1600	145	145

It is apparent from Table 2 that in a single satellite network:

1. For a specific satellite, the power capacity of a single satellite network is determined mainly by the G/T values of the ground stations in the network and the form of modulation employed.

2. For the same satellite, there is an optimal relationship among ground stations, forms of modulation, and network capacity. Full utilization of network power and frequency band is attained under these conditions. For example, single networks composed of ground stations and a single satellite with $(G/T)_E$ = 25.8dB/K when using $\Delta M/2\phi$-PSK and $(G/T)_E$ = 31.28dB/K when using $\Delta M/4\phi$-PSK are optimal networks.

3. When the G/T value of a ground station exceeds the optimal state, the network is in a state of restricted satellite frequency band. The network bandwidth is insufficient and there is excess power, so the cost effectiveness of the network would be low.

4. When the G/T value of a ground station is less than the optimal state, the network is in a state of satellite power restriction. Network power is insufficient, there is excess frequency band, and the cost effectiveness of the network also would be low.

It is apparent that for specific satellites and forms of modulation, a single satellite network should select an appropriate ground station to achieve an optimal network state.

2. Mixed satellite networks

In principle, many types of ground stations can form a mixed satellite network. Like a simple network, network capacity also depends on network bandwidth capacity N_B and power capacity N_P. Still, the power capacity N_P relationships of a mixed satellite network are rather complex. Below, we will study two common types of mixed satellite networks.

1) A mixed satellite network composed of two different types of ground stations

In this type of network, because ground stations with two different G/T values have different satellite power requirements, changes also occur in the network power capacity N_{PII}, but these can be extrapolated according to basic principles to:

$$N_{PII} = A^{-1}n_L - (k_S-1)N_S$$

In the formula, n_L is the power capacity when a large ground station in a network corresponds to a single network,

N_S is the number of carrier waves received by a small ground station $(0<N_S<P_P/AP_S)$,

k_S is the ratio between the satellite power P_S required for each carrier wave when receiving at a small ground station and the satellite power P_L required for each carrier wave when receiving at a large ground station,

P_P is the equivalent isotropic radiated power of the satellite,

A is the carrier wave excitation factor.

Obviously, by using the above formula to derive a required value for N_S in $0<N_S<P_P/AP_S$, we can compute N_{PII}, and by comparing N_{PII} with N_B, we can derive N_{II}.

Based on the definition of an optimal network, the optimal capacity of a satellite network composed of two types of ground stations can be derived using the following formula:

$$N_S = \frac{P_P - N_B \cdot A \cdot P_L}{A(P_S - P_L)}$$

$$N_L = N_B - N_S$$
$$N_{II} = N_L + N_S$$

In the formula, N_L is the number of carrier waves received by a large ground station in a mixed network, and P_L is the satellite power required for each carrier wave when receiving at a large ground station.

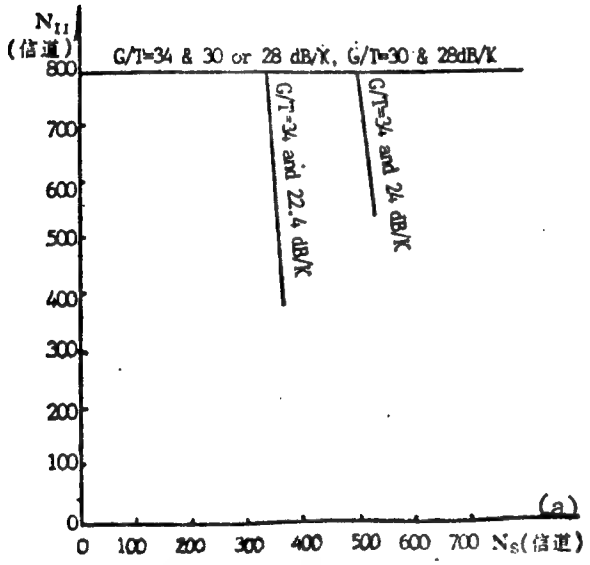

Figure 5. Capacity of a Mixed Satellite Network Composed of Two Types of Ground Stations Using $\Delta M/2\phi$-PSK Modulation

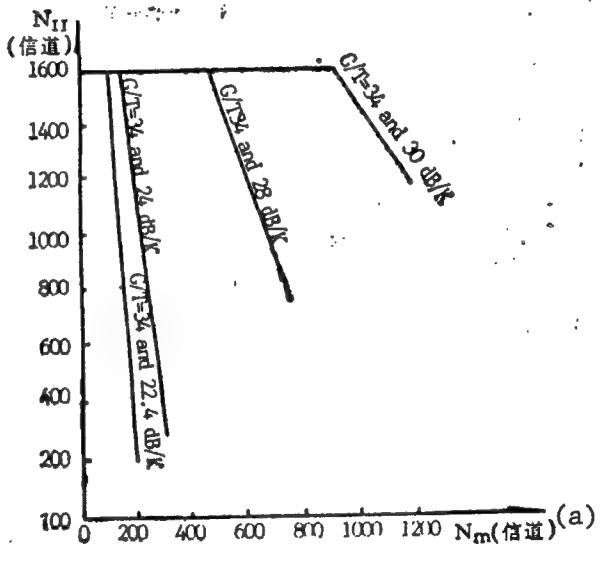

Figure 6. Capacity of a Mixed Satellite Network Composed of Two Types of Ground Stations Using $\Delta M/4\phi$-PSK Modulation

Key: (a) channels
Satellite EIRP = 28dBW
N_{II}: Satellite network capacity
N_S: Number of carrier waves received by a small ground station

Figures 5 and 6 provide examples of this type of network. It is apparent from the graphs that when a small ground station is receiving a rather small number of carrier waves, network capacity is at a maximum as shown by

the lines parallel to the horizontal axis. At this time, the frequency band is restricted and network power is wasted. When the number of carrier waves received by a small ground station is increased to the point where the line bends, the network's $N_{PII} = N_B$, which is an optimal state. Past the bend, network capacity declines as the number of carrier waves received by a small ground station increases, i.e., $N_P < N_B$. At this time, power is restricted and there is excess frequency band.

2) A mixed satellite network composed of three types of ground stations

This is a common type of network used for domestic satellite communications. A network with ground stations having three different G/T values is more complex, but the basic principles are identical to those in a mixed network composed of two types of ground stations. Its power capacity has the following relationship:

$$N_{PIII} = A^{-1}n_L - (K_M - 1)N_M - (k_s - 1)N_s$$

In the formula, N_M is the number of carrier waves received by an intermediate-sized ground station in a mixed network.

K_M is the ratio between the satellite power P_M required for each carrier wave when receiving at an intermediate-sized ground station and the satellite power P_L required for each carrier wave when receiving at a large ground station.

It is apparent in the formula that N_{PIII} is a function of N_M and N_s. To compute N_{PIII}, we first must determine N_M and N_s. We know form basic principles that:

a) When N_s in $\frac{P_p - N_B \cdot A \cdot P_L}{A(P_s - P_L)} < N_s < \frac{P_p}{AP_s}$, N_M should be chosen within the range $0 < N_M < \frac{P_p - N_s AP_s}{AP_M}$

b) When N_s in $0 < N_s < \frac{P_p - N_B \cdot A \cdot P_L}{A(P_s - P_L)}$, N_M should be chosen within the range

$$0 < N_M < \frac{P_p - N_s A(P_s - P_L) - N_B AP_L}{A(P_M - P_L)}$$

For the same reason, based on optimal principles, when a mixed-network composed of three types of ground stations is within the range

$$0 < N_s < \frac{P_p - N_B \cdot A \cdot P_L}{A(P_s - P_L)}$$

there is a corresponding optimal capacity for each N_s. Thus, within this range, the selection of the required N_s can be derived by the steps shown in the following example,

$$N_M = \frac{P_p - N_s A(P_s - P_L) - N_B A P_L}{A(P_M - P_L)}$$

$$N_L = N_B - N_M - N_s$$
$$N_{III} = N_L + N_M + N_s$$

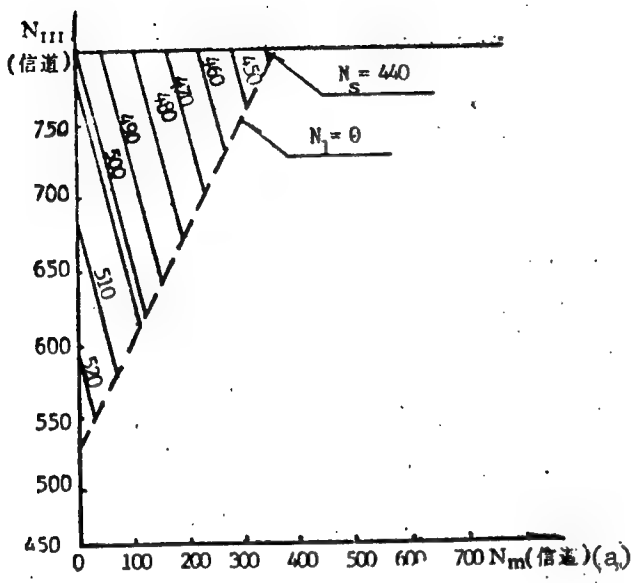

Figure 7. Capacity of a Mixed Satellite Network Composed of Three Types of Ground Stations Using ΔM/2ϕ-PSK Modulation

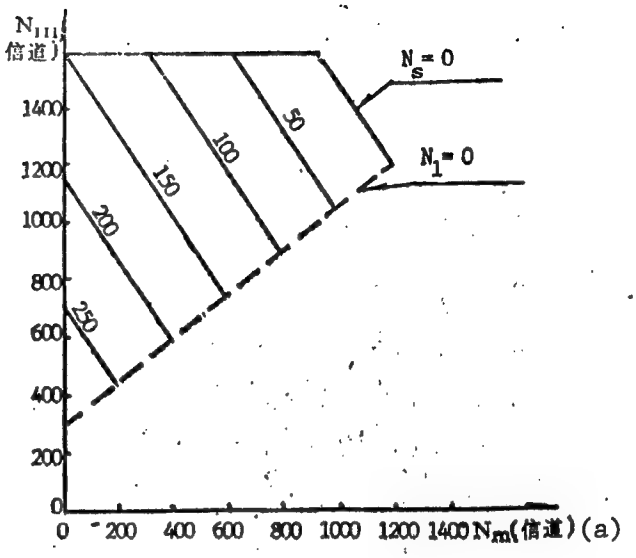

Figure 8. Capacity of a Mixed Satellite Network Composed of Three Types of Ground Stations Using ΔM/4ϕ-PSK Modulation

Key: (a) channels
Satellite EIRP: 28dBW
Ground station (G/T) = 34, 30, 24dB/K
N_{III}: Satellite network capacity
N_s, N_M, and N_L: Respectively, the number of carrier waves received by small, intermediate-sized, and large ground stations

Figures 7 and 8 illustrate examples of this type of network. It is apparent from the figures that the slanted line which intersects the maximum values on the vertical axis is a boundary. Below and to the left of this line, all combinations of numbers of carrier waves received at three types of ground stations cause the network to be in a state of restricted power, and there is a severe crop in network capacity. Above and to the right of this line, however, it is possible for the network to be in a restricted power, restricted frequency band, or optimal state depending on the combination of numbers of carrier waves for the three types of ground stations.

Figures 7 and 8 illustrate a situation using different forms of modulation in the same type of satellite network. It is apparent that the optimal capacity of the latter network is about double that of the former, and that the total investments in each of the two types of networks are basically identical, so economic efficiency in the latter network is much higher than in the former. It is apparent from this that forms of modulation play a major role in mixed satellite network performance.

IV. Conclusion

In summary, in satellite communications, satellite network capacity depends on power capacity and frequency band capacity. The capacity of a mixed network composed of different types of ground stations falls between that of a single network capacity corresponding to small ground stations and large ground stations. Within this range, there can be any number of combinations of number of carrier waves for each type of ground station in the network, and network capacity changes with the combinations. For a specific satellite and ground station, maximum network capacity depends on the form of modulation employed. For a specific satellite and form of modulation, network capacity in a single network varies according to the G/T values of the ground stations, while in a mixed network it varies not only with ground station G/T values but also with changes in the combination of numbers of carrier waves received by each type of ground station. For a specific ground station, with small ground stations receiving different numbers of carrier waves, there are different combinations of numbers of carrier waves received by each type of ground station. Three states can exist in any type of satellite network:

1) An optimal state. Network power capacity and frequency band capacity are equal and there is full utilization of satellite power and frequency band. Network capacity reaches a maximum value, network efficiency is at its highest, and economic results are optimal.

2) A frequency band restricted state. There is excess network power but insufficient frequency band. Network capacity can be similar to that in the "optimal state" but full utilization of satellite power or ground station G/T values is not achieved, leading to waste and poor economic efficiency. Improvement to attain an optimal state can be achieved by reducing ground station G/T values, using satellites with less power, or adopting forms of modulation which can make full use of the satellite frequency band.

3) A power restricted state. There is excess network frequency band but insufficient power. The result is waste of network frequency band and a sharp decline in network capacity. The maximum capacity in the two states described above cannot be attained, which causes low network efficiency and poor economic results. In this situation, satellite power can be increased, the G/T values of small ground stations can be increased, or the number of carrier waves received by small ground stations in the network can be reduced. Where capacity permits, forms of modulation which can make full use of satellite power also can be adopted. All of these will lead to improvements and permit the attainment of an optimal state.

In summary, the first state is the goal of satellite network designers while the latter two states should be avoided. In reality, a satellite network should operate in a situation of excess power and frequency band to facilitate network expansion. Network design, however, should begin with an optimal situation.

12539/9365

Design of PFM Modulator for Color-TV PFM-IM Fiber-Optic Transmission System

40080119b Beijing DIANZI JISHU YINGYONG [APPLICATION OF ELECTRONIC TECHNIQUE] in Chinese No 3, Mar 88 pp 27-30

[Article by Geng Tianshou [5105 1131 1108] of Shanxi University: "Engineering Design of a PFM Modulator in a PFM-IM System Fiber-Optic Transmission System"]

[Excerpts] A broad-range highly linear pulse frequency modulator is the core of a PFM-IM system color TV fiber-optic transmission system. The use of PFM-IM for fiber-optic transmission of color TV signals provides low distortion, a high transmission signal-to-noise ratio, long transmission distances, and suitable system creation costs, so it has attracted attention in China and other countries. The pulse fiber-optic modulator in such a system plays an important role in system indices. This article will outline working principles, design principles, an engineering design method, and an example design.

III. Modulator Engineering Design

Design of a PFM-IM color TV fiber-optic transmission system begins with proposed transmission indices, the main ones being degree of distortion and signal-to-noise ratio. When these indices are given, concrete requirements for each system component can be proposed. The main requirement for a pulse modulator is excellent linearity of Vc-f characteristics to reduce nonlinear distortion. Frequency deviation should be great to attain a high transmission signal-to-noise ratio. The center frequency cannot be too low, to prevent mixing of higher-order modulation pulse harmonics with baseband signals, which creates distortion. The ultimate task of modulator engineering design is to obtain the range of linear pulse frequencies $f_1 \sim f_2$ at an input signal amplitude of ΔVc. A design of a modulator based on this requirement follows.

1. Circuit structure

Circuit structure principles were the basis for selecting the example circuit arrangement in Figure 3. ECL [emitter coupled logic] circuits are used for IC_1 and IC_2.

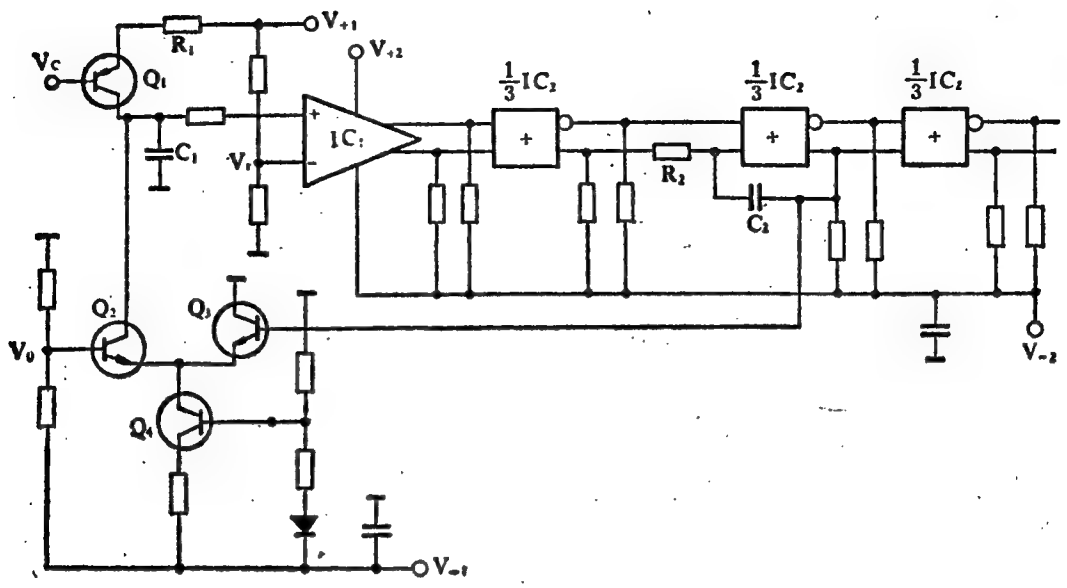

Figure 3.

2. Determining primary parameters

1) Determining V_0

The base voltage of Q_3 is the monostable ECL level V_{OH} and V_{OL}, i.e.,

$$V_0 = \frac{V_{OH} + V_{OL}}{2} \tag{14}$$

2) Determining sawtooth voltage amplitude V_{C1} and comparator reference voltage Vr.

A comparator usually has a several-millivolt region of blurring. A sawtooth voltage in this region places the comparator in a zone of amplification, which creates left/right fluctuation in the position of the monostable output pulse, so it is best if the sawtooth voltage amplitude is somewhat greater, usually $|V_{C1}|>1V_{p-p}$, and Vr can be determined from this.

3) Determining output pulse width of a monostable circuit t_d.

Near the maximum oscillation frequency, the pulse duty cycle is at a maximum, with $\delta \approx 50$ percent. To ensure excellent linearity at the high end of the working frequency band, the duty cycle at f_2 should not be too great. It usually is best to set δ = 20 to 30 percent. Thus,

$$t_d = T_2\delta = \delta/f_2 \tag{15}$$

T_2 in the formula is the period at frequency f_2. This can be used to derive the time constant R_2C_2 of the monostable circuit.

3. Determining primary component values

1) Determining i_d

A discharge constant-current source usually is made up of low-power UHF transistors with I_{CM} in the range of several milliamps, so it is best if i_d is not too large. It usually is best to choose 15 ~ 20 mA. At this time, the minimum charging current also is not too small. After selecting i_d, a discharge constant-current source and switching switch circuit can be designed.

2) Determining C_1

This is determined on the basis of a frequency of f_2:

$$Q_{charged} = C_1 |V_{C1}| = is_2 (T_2 - t_d) = is_2 \frac{1-\delta}{f_2} \tag{16}$$

From formula (5) $is_2 = f_2 i_d t_d = i_d \delta$ (5')

Inserted into formula (16):

$$C_1 = \frac{i_d \delta (1 - \delta)}{|V_{C1}| \cdot f_2} \tag{17}$$

3) Determining R_1

From formula (5) $\Delta f = f_2 - f_1 = \frac{\Delta is}{i_d t_d}$ (18)

From Figure 3

$$is = \frac{V_{+1} - V_C - V_{BE}}{R_1} \tag{19}$$

or $$\Delta is = is_2 - is_1 = \frac{\Delta V_C}{R_1} \tag{20}$$

From formulas (18) and (20)

$$R_1 = \frac{\Delta V_C}{i_d t_d \Delta f} \tag{21}$$

4) Determining the Q_1 base voltage

The results of the above calculations indicate that there must be an appropriate working point for the base of Q_1 to ensure that the required frequency range is attained at the provided input signal amplitude. It usually is set via a clamping circuit with a potentiometer to adjust the clamping level.

a) Q_1 base level V_{C2} at f_2:

From formulas (19) and (5') we have

$$V_{C2} = V_{+1} = i_d \delta R_1 - V_{BE} \tag{22}$$

(b) Q_1 base level V_{CB} at f_B:

$$V_{CB} = V_{C2} + \frac{1}{2} V_f + V_{sync} \tag{23}$$

V_f in the formula is the amplitude of the modulated signal of the simultaneously transmitted audio, data, and other signals. V_{sync} is the amplitude of synchronous signals.

4. Example

Design a pulse frequency modulator with an input baseband signal amplitude of $1.422V_{p-p}$ (including a video signal of $1V_{p-p}$, V_{sync} = 0.3V audio, and a total data modulation signal amplitude of $0.186V_{p-p}$) and a frequency range of 25 ~ 45 MHz.

1) Selecting circuits and components

In selecting the circuit in Figure 3, IC_1 is a J685, IC_2 is an E10105, Q_1 is a 3CK2B, and Q_2 ~ Q_4 are 3DG80.

2) Determining V_0: from formula (14), V_0 = -1.2V.

3) Determining $|V_{C1}|$ and Vr: assuming that $|V_{C1}|$ = 1.2V, it is apparent from Figure 3 that when Q_2 is conducting, $V_{CE} \approx 0.7V$, so Vr $\approx$ 0V.

Practice has proven that the highest oscillation frequency in monostable circuits composed of several E10105s can be attained when V_0 = -1.1V, so Vr $\approx$ 0.1V. It is supplied by a resistance voltage divider.

4) Determining t_d:

From formula (15) we have:

$$t_d = \delta / f_2 = \frac{0.25}{45 \times 10^6} = 5.6\text{ns}$$

5) Estimating the maximum oscillation frequency f_{max}

Measured $t_1 = t_4$ = 6ns, t_2 = 3ns, and t_3 = 1.5ns.

From (13) we obtain f_{max} = 52.4MHz,

The measured f_{max} is 52 ~ 56.5MHz, so component selection is feasible.

6) Selecting i_d: i_d = 15mA

7) Determining C_1:

From formula (17) we derive C_1 = 52pF, so the standard value of 51pF can be used.

8) Determining R_1:

From formula (21) we derive R_1 = 846Ω, so a 1 kΩ potentiometer can be used.

9) Q_1 base blanking level V_{CB}

From formula (22) we derive Vc_2 = 2.13V, (when V_{+1} = 6V).

From formula (23) we derive V_{CB} = 2.53V

Design completed.

An experimental circuit was prepared according to the above design circuit and values,

$$V_{+1} = V_{+2} = 6V,$$

$$V_{-1} = V_{-2} = -5V,$$

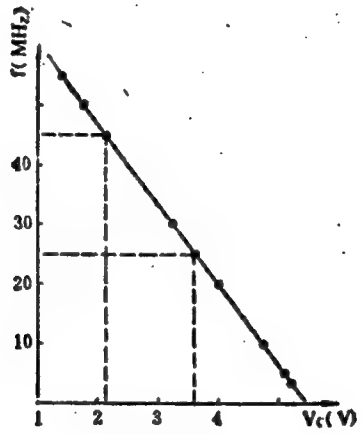

Figure 7.

Careful circuit board design and insertion of a small 51 ~ 100Ω resistor at the input end of the comparator eliminated high frequency micro-oscillation in the input sawtooth voltage waveform of the comparator and improved modulator performance. The measured Vc-f characteristics are shown in Figure 7. Oscillation frequency is 0.4KHz ~ 56.5MHz, which conforms well to the calculations in the working frequency band. This modulator is being used for PFM-IM color TV video and audio, and in 10kbit/s-and-under data transmission systems.

Practice has proven that in a circuit designed by this method, attaining the required frequency deviation range merely requires that the regulated clamping level reach the calculated value, making modulation convenient and repeatability excellent.

References

1. Zhu Xiaogen [2612 1420 2704], "A Fiber-Optic Transmission System for Color TV Signal PFM-IM Systems," DIANSHI JISHU [TELEVISION TECHNOLOGY], No 6, 1985, pp 22-26.

12539/9365

Far-Field Measuring Methods, Instruments for Fiber-Optic Numerical Aperture

40080119c Shanghai DIANZI JISHU [ELECTRONIC TECHNOLOGY] in Chinese Vol 15, No 2, Feb 88 pp 2-3

[Article by Liu Chaoding [0491 2600 7844]: "Far-Field Measurement of Fiber-Optic Numerical Aperture and Instruments"]

[Excerpts] Far-field measurement of the numerical aperture of optical fibers is a quick and effective measurement method that has developed gradually since the late 1970's. In the past, most measurements of this basic parameter of multimode optical fibers were made via the light spot method. Although convenient, the precision of measurement and resolving power were poor. A refraction near-field method also was used which involved first measuring the distribution of refractivity in the optical fibers and then computing the numerical aperture. Measurement was rather difficult, however, and usually suited only to the laboratory. The advantages of far-field measurement are simple operation, greater precision, and greater resolving power, and it is attracting increasing attention in many countries. It was included among CCITT proposals in 1984 and recommended. In China, the Chinese Academy of Sciences' Shanghai Silicate Institute was the first to develop this type of measurement equipment successfully. Later, on this foundation, the Posts and Telecommunications Engineering Equipment Plant developed the "GC-1 Fiber-Optic Dissipation Far-Field Measurement Instrument" and pushed this measurement technology a new step forward toward instrumentation and utilization.

II. Principles of Far-Field Numerical Aperture Measurement

Based on the CCITT proposals, the largest theoretical numerical aperture is defined as

$$NA_{(t\ max)} = \sqrt{n_1^2 - n_2^2} \qquad (3)$$

In the formula, n_1 is the maximum refractivity of the fiber core and n_2 is the refractivity of the innermost cladding.

By measuring n_1 and n_2, we can calculate $NA_{(t\ max)}$, but the measurements are rather difficult.

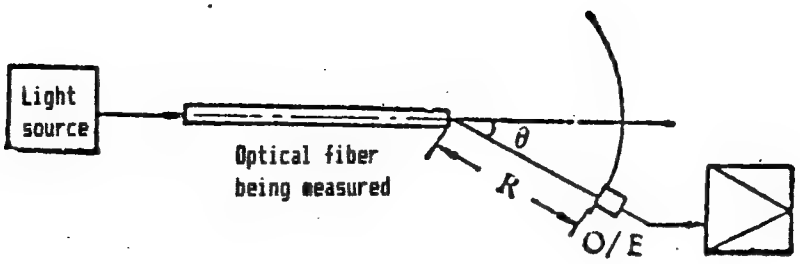

Figure 2. Principles of Far-Field Measurement

The principles of far-field measurement are shown in Figure 2. A light source transmits light into the optical fiber via a coupling at one end. Lambert excitation also is necessary. The light then radiates from the other end of the fiber. A detector scans a circular arc at site R (R << the fiber core diameter) at the far radiating end of the fiber, measures the intensity of the radiated light (the unit solid angle luminous power) at an angle θ off-center from the axis of the fiber, and displays the distributional curve $P(\theta)$ of the light intensity at various angles θ on a CRT screen. When the detector is aligned exactly with the axis of the fiber, $\theta = 0$ and the measured $P(0) = P(\theta)_{max}$. As the detector is moved gradually away from the axis of the fiber, the measured $P(\theta)$ value gradually decreases. When the luminous power drops from P(0) to 0.01P(0) or 0.5P(0), the angle from the axis of the optical fiber is $\theta_{0.1}$ or $\theta_{0.05}$, and the measured numerical aperture is

$$NA_F \approx \sin \theta_{0.1} \text{ (or } \sin \theta_{0.05}) \quad (4)$$

According to theoretical deviations, for GI optical fibers,

$$NA_{F0.1} \approx 0.95NA_{(t\ max)}$$

and for SI optical fibers,

$$NA_F \approx NA_{(t\ max)}$$

III. Structure of a Far-Field Tester

A far-field tester is composed of a light source, rotating scanning detector disk, image display. numerical aperture angle counter, and other parts. A block diagram of the principle is shown in Figure 3.

1. Light source

The light component is a bromine-tungsten bulb. Besides producing white light, changeable filters also can produce quasi-monochromatic light (with a spectral halfwidth of $\leq$10nm) at wavelengths of 0.85μm or 1.3μm, and by using a mechanical chopper, it can output 270Hz chopped light to reduce interference by external light. The light path system is shown in

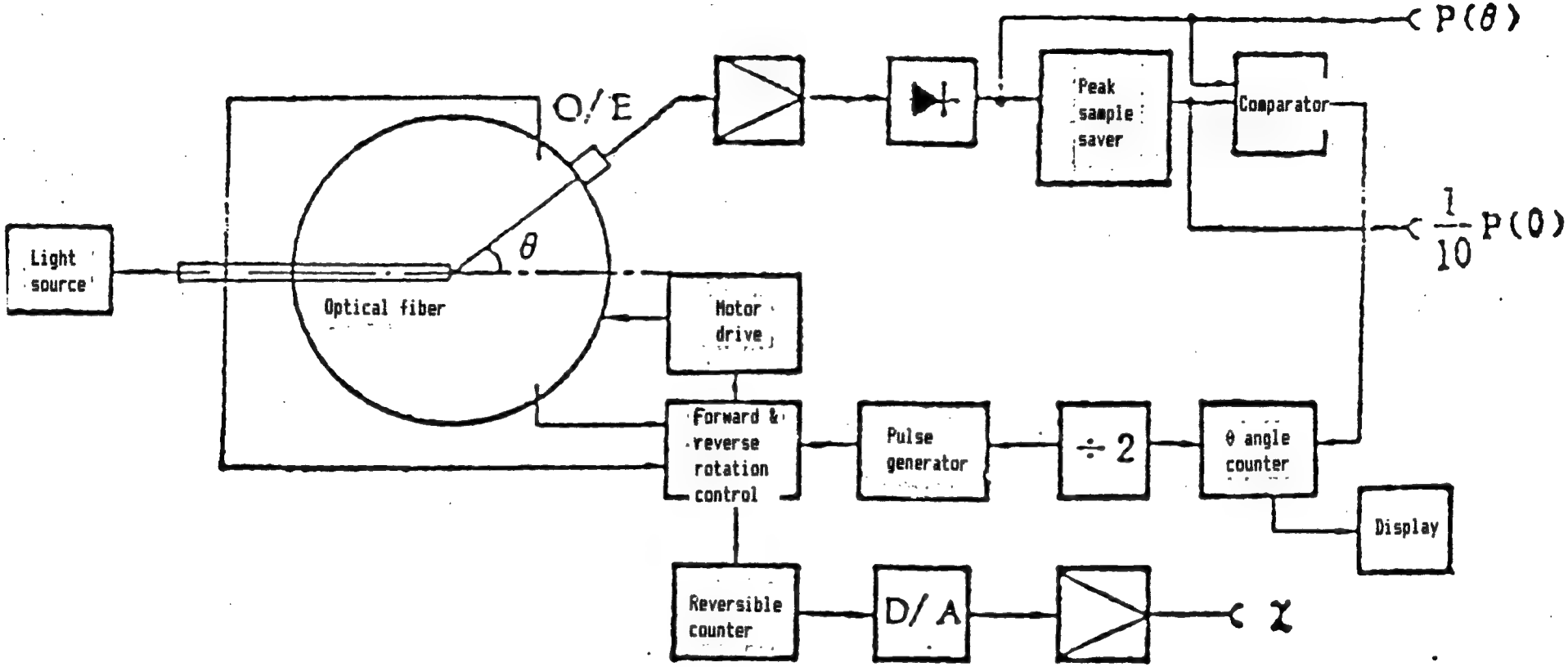

Figure 3. Block Diagram of Far-Field Measuring Device

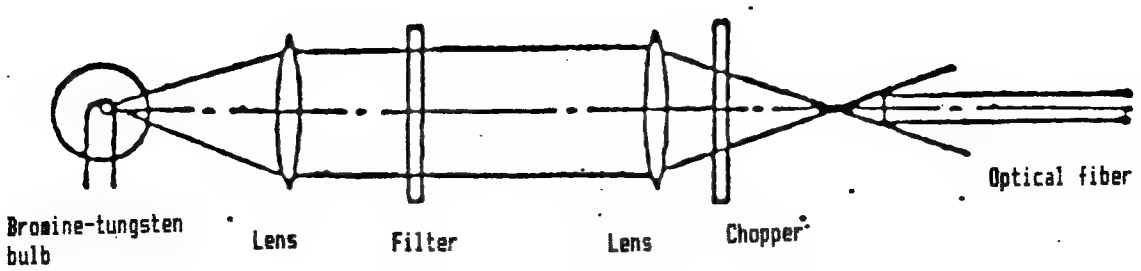

Figure 4. Light Path System

Figure 4. The center line of the light path must be aligned precisely with the axis of the fiber. The end of the fiber is located near the focal point of the lens. The light spot from the light source at the end of the fiber is larger than the end of the fiber. Moreover, the light cone of the light source is larger than the numerical aperture angle of the fiber being measured to assure full excitation of the fiber by the light source.

2. Rotating scanning detector disk

Scanning is done via an arrangement using a fixed optical fiber and a detector which rotates around the end of the fiber. The detector is driven by a stepping motor with one measurement for every 0.1° of rotation. The angle of rotation and the luminous power at each site also are recorded simultaneously to provide primary data on the image display and to compute the numerical aperture. The circular arc scanned by the detector should be located on the flat surface passing through the axis of the fiber so that the measured $P(\theta)$ curve can reflect the far-field light intensity distribution radiated from the meridian line of the end of the fiber. For this reason, during the tests, the fine tuning rack used to hold the fiber and the coupling between the light source and fiber should be readjusted repeatedly, first to achieve a maximum P(0) value and then for scanning detection. To test optical fibers with large numerical apertures, the range of rotation of the detector can be ±25°. A contact is installed at the angle of maximum rotation to control the forward and reverse rotation of the electric motor.

3. Image display and computation of numerical aperture angle

An image like that shown in Figure 5 is displayed on the CRT screen. The horizontal axis represents the θ value and the vertical axis represents the luminous power. The solid line on the screen represents the measured $P(\theta)$ curve and the horizontal dashed line is the angle representation curve. The points of its intersection with the $P(\theta)$ curve are determined by a P(0) of 0.1 (or 0.05) and can be chosen artificially. Each dash and each space in the dashed line represent 1°. During the scanning process, when the $P(\theta)$ value drops to a P(0) of 0.1 (or 0.05), the $P(\theta)$ curve intersects the angle representation line. The number of dashes in the angle representation line between the intersection of the dashed and solid lines represent degrees of numerical aperture.

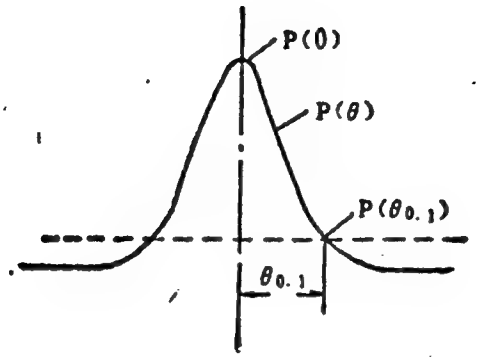

Figure 5. CRT Image Display

4. Block diagram of working principles

It is apparent from the block diagram in Figure 3 that the pulse from the pulse generator drives the rotation of the stepping motor, is transmitted to a reversible counter for counting, and passes through the D/A converter to create a triangular wave corresponding to the scanning, which is displayed as x-axis signals on the image display. The y signals for the $P(\theta)$ curve are obtained from the light signals measured by the detector after amplification. The angle representation line signals are obtained by sampling the peak $P(\theta)$ signal values to maintain the circuit at P(0) and then increase it to 0.1 (or 0.05).

The numerical aperture angle is counted by the number of pulses to the counter gate and the drive motor. By sending the $P(\theta)$ signals and angle representation line signals simultaneously to the comparator, when the $P(\theta)$ signals pass through the angle representation line, an abrupt change occurs in the comparator output, which then creates the counter gate signals. Because the gate width is double the required width, pulses going to the drive motor are divided by two and then sent to the counter. This permits direct reading of the numerical aperture angle at a resolution of 0.1°.

5. The question of measurement precision

To improve measurement precision, consideration was given to instrument design in these areas: 1) There must be stabilized light sources and accurate light path systems to satisfy the Lambert excitation conditions of the optical fibers; 2) Notice must be taken of the time constant of peak value sampling to maintain the circuit and the scanning speed to obtain correct angle representation line signals; 3) There must be a reliable light coupling component and fine tuning device; 4) The angle counter, image display, and actual rotational position of the electric motor must be synchronized. The main aspects of the measurements are the manufacture and inspection of the end surface of the fiber, while operation is rather simple. If there are defects in the end surface of the fiber or if it is not perpendicular to the axis of the fiber, measurement errors may result. Inspection of the quality of the end surface of the fiber usually requires

that it be examined under a microscope, which is somewhat time-consuming, but it is rather easy to see it clearly in the image of the $P(\theta)$ curve. The reason is that any defect in the end surface will create anomalies or asymmetries in the displayed $P(\theta)$ curve. First examining the image of the $P(\theta)$ curve and then measuring the numerical aperture not only can avoid unnecessary increases in the precision of measurement but also can greatly improve testing efficiency. In addition, the $P(\theta)$ curve also can be used to determine if transmission by the optical fiber is stable or not, which is very important for ensuring precision when measuring losses in the fiber.

Numerous measurements with this instrument have confirmed a repetition error of less than 0.5 percent, which is a considerable improvement over the design index of 5 percent. In actual measurement, the maximum error between the measured value of optical fibers produced by the Corning Company in the United States and their stated values was less than 0.004.

References

1. CCITT Proposals (Redbook), G.651.

2. Zhang Xu [1728 3563] GUANGXIAN TONGXIN YUANLI [PRINCIPLES OF FIBER-OPTIC COMMUNICATIONS].

12539/9365

On Trends of Development of Local Telephone Networks Re Optical Cable, ISDNs

40080140 Shanghai DIANXIN KUAIBAO [TELECOMMUNICATIONS INFORMATION] in Chinese No 3, Mar 88 pp 21-29

[Article by Xu Naiying [1776 0035 5391]: "On the Developmental Trends of Local Networks in China"]

[Excerpts] Abstract: This article examines the developmental trends of local networks in China, from the standpoints of local telephone network organization, trunk-line networks subscriber line networks, data networks, special use networks and integrated services digital networks (ISDN). It also briefly discusses the application of optical cable to local networks.

5. The Application of Optical Cable

In recent years, due to the rapid development of fiber-optic communication technology and the large-scale application of digital switching, there has been wider use of optical cable in local repeater networks. The chief advantages of optical cable are: (1) the large capacity of fiber-optic communications is suitable for large-capacity trunk lines between digital bureaus; (2) single-mode fiber-optic systems are improving daily, with greater reliability and lower cost, so that their application has gone from long distance to localities; (3) fiber-optic communications systems which do not cover long distances do not require instruments installed in manholes; (4) optical cables are of small diameter and light weight, which saves on pipeline and is cheaper to lay at long lengths; (5) optical cable is not subject to interference from bursts of electricity.

The multimode, graded-index optical cable initially used in trunk lines worked at a wavelength of 0.85 micrometers and was gradually developed to work at a wavelength of 1.3 micrometers. Accompanying the increased speed of transmission were rapid developments in single-mode optical fibers. At present, the attenuation and badwidth (or dispersion) of single and multimode optical fibers at 1.3-micrometer wavelength are approximately as illustrated in Table 1.

TABLE 1: Transmission properties of optical fibers at a wavelength of 1.3 micrometers

Property	Categories of Optical Fibers	CCITT[11] Ordinary Quality	CCITT[11] High Quality	Domestically Produced Ordinary Quality	Domestically Produced High Quality
Attenuation dB/km	Multimode	< 2	0.5~0.8	< 2	0.5~0.8
	Single Mode	< 1	0.3~0.4	< 1	0.4~0.6
Bandwidth MHz.km	Multimode	> 200	> 2000	400~500	> 1000
Dispersion ps/nm.km	Single Mode	< 3.5		< 6	< 3.5

The Consultative Committee on International Telegraphy and Telephony (CCITT), based on the 1984 standards for light sources and receivers, recommended that the permissible attenuation (see Diagram 5) between transmitter (S) and receiver (R) be as illustrated in Table 2. This includes both fiber and connection losses. It also includes that calculated as likely to occur during the period of operation due to route change and increased contact, as well as residual Mc.

Assuming a relatively constant numerical value of 1.0 dB/km for the fiber-optic attenuation, then attenuation at the point of contact is 0.3 dB/km and Mc is 0.3 dB/km, for a total of 1.6 dB/km. From this it is possible to calculate the relay intervals under various conditions. Again, if we assume a bandwidth cluster value of 0.8, it is then possible to calculate from the above relay interval the required fiber-optic bandwith. The results of these calculations are shown in Table 2.

In the past few years, the developmental trend in optical devices has been to make use of the increased attenuation between sender and receiver. When a laser device is used as the light source, at speeds of 34 Mb/s [DS 3] and 140 Mb/s [DS 4], some commercial products can differ as much as 38 and 32 dB. So by using attenuation as a starting point, the relay interval can be increased even more. It is worth noting that when the 140 Mb/s speed is used, the bandwidth becomes a limiting factor. Domestically produced multimode optical fibers can accomplish what is illustrated in Table 2 for 960 MHz·km, an end rate that is still low.

But in any case, when speaking of the great majority of trunk lines between stations, it is possible to do without regenerative devices. Trunk lines which perform well at specific intervals can also be equipped with relay devices at stations en route.

FIGURE 5: Structure of a fiber-optic communication system

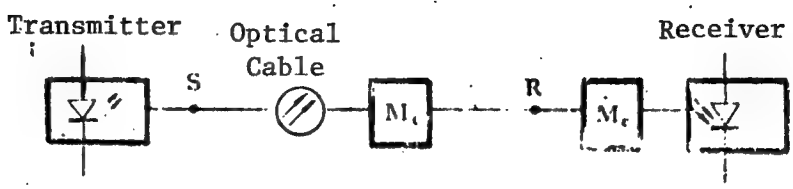

M_c: Loss in the Cable M_e: Loss in equipment

TABLE 2: Characteristics of multimode fiber-optic transmission between transmitter and receiver, and examples of its calculated relay interval and bandwidth requirements

Rate: kilobits per second (kb/s)	Category of light source	Characteristics between transmitter & receiver (CCITT)		Calculated examples	
		Attenuation in dB	3dB optical bandwith in MHz	Relay interval in km	Fiber-optic bandwidth in MHz·km
34,368	Laser device	35	50	21.9	591
	L D	22	50	13.8	408
39,214	Laser device	27	100	16.9	960
	L D	18	100	11.3	696

Due to the development in the past several years of single-mode fiber-optic technology and coupling technology, the price of single-mode systems is close to that of multimode systems. Therefore, in trunk lines of larger service capacity, especially where there might be an increase in routing to 565 Mb/s, choice of the single-mode fiber-optic design can be appropriate. The CCITT has not yet formally established properties for single-mode systems between transmitter and receiver. The properties illustrated in Table 3 were recommended by the XVth Research Group's October 1986 meeting.[12]

TABLE 3: Characteristics of single-mode optical fibers between transmitter and receiver at a wavelength of 1.3 micrometers

Rate in kilobits per second kb/s	Category of light source	Characteristics between transmitter & receiver	
		Attenuation in dB	Dispersion in ps/nm
139,264	Laser device	28~31	300~360
4×139,264	Laser device	22~26	90~120

A comparison of Tables 1 and 3 shows that at present domestically produced single-mode optical fibers can be regarded as of satisfactory quality in DS 4, but in DS 5 chromatic dispersion still requires some attention.

To summarize the foregoing, local network trunk lines which use light sources can employ DS 4 multimode, long-wave optical cable or single-mode optical cable. Certain large-service trunk lines can appropriately select single-mode optical cable. Due to the large communications capacity of optical cable, it is very important to ensure its safe operation. For this reason, there needs to be a backup system, and important relay cable will be double routed. If the cable is routed through an alternate station, as much of it as possible should enter the station, and a ring installation employed for the optical wire, in order to increase mobility. The optical cable which enters the station should not be composition cable, in order to decrease connectors and increase reliability.

Because optical cable has a small diameter, there is a savings on tubing, so it is easier to construct and to ensure the safety of the light source. In the 90-mm-internal-diameter concrete tubing frequently used in China, there can be 3-4 of the 34-mm-external-diameter polyethylene plastic tubes. The polyethylene tubing's friction coefficient is about 40 percent that of the concrete tubing. Adopting this kind of tubing can result in a savings on each tube's internal loss, decreasing the latter from approximately 10,000 yuan to 5,000 yuan per kilometer.

Integrated Services Digital Networks (ISDN)

Along with the development of computer technology and digital communications technology, the various information services can readily employ digital signals for display and transmission. Therefore they could use a digital network to assume various functions, including internal telephones.

China's telephone network is still underdeveloped, so our first step must be a strong effort to develop this network. Expanding the telephone's dissemination and level of automation are basic to this. It is currently limited to national power; it is not possible to extend the transition to ISDNs to a national scope. But there should be research into this area. There also can be small-scale tests conducted in a few localities. In addition to this small-scale testing, China's development of ISDNs should be implemented in three separate steps:

1. Integrated Digital Networks (IDN).

This will involve converting from analog to digital those transmission lines which are for switching and other than consumer use. At this stage there must still be a distinction between the two major categories of telephone and non-telephone nets, unique systems which cannot communicate with one another. However, the next step will employ a digital network to create the conditions for carrying out various services.

2. Narrow-Band ISDN

Because of the large investment required by subscriber line nets, this stage will require the continued use of the original subscriber lines, i.e., copper cable networks. This is economically advantageous. Based on the acoustical mixing and attenuation of the subscriber cable which now exists, the CCITT recommended that at the limits of bandwidth and distance, a 2B+D channel be used for transmission. B is a channel of 64 kb/s, which can transmit a telephone signal or a non-telephonic service below 64 kb/s. D is a 16 kb/s channel, used for transmitting signals and groups of data. The total is 144 kb/s, which is termed basic access. If some synchronizing and controlling codes are added to this, bringing the total to about 160 kb/s, it is termed the U port, and uses two lines to link up with the subscriber. The two-line transmission is accomplished by two methods: one is by time compression multiplexing (TCM), also called the ping-pong method, in which half of the time is devoted to transmission, and the other half to reception, thereby doubling the rate. The other is the echo cancellation method, whereby transmission and reception are

carried out simultaneously, using digital storage technology to cancel out the echo. Each has its good and bad points; the majority trend is toward the latter method, but it is still in the developmental stage. There is as yet very little research on this subject in China.

3. Wideband ISDN

Transmission here of a 30B+D signal is via an approximately 64 kb/s channel. 30B can be used to transmit voice, images or data signals below 1920 kb/s. D is used for common-channel signaling and data packets, with a total transmission rate of 2048 kb/s. As it turns out, it is one to a digital standard transmission rate, so that it becomes a DS 1 primary access. The wide-band signal uses four lines for transmission, and if it still uses copper cable to transmit then two opposing lines are required. Because copper cable is subject to the limitations imposed by near-end sound mixing and attenuation, the relay interval can still make use of only part of the line, so that as the number of wide-band users increases, there will naturally be a steady transition to optical cable.

In the past several years, due to the development abroad of new services, especially such as database services, computer networks, pay-television, etc., DS 1 primary access has been rendered obsolete, as transmission rates have climbed steadily, reaching 30-45 Mb/s and even as high as 120-140 Mb/s. Under these circumstances, only optical cable will do for transmission.

General use of optical cable in domestic subscriber networks is still some time in the future, but it is possible for special networks to make use of it. In the initial stage of subscriber use of optical cable, many nations have emphasized the choice of large-core, multimode optical fibers, so as to increase the light source's coupling rate of efficiency and make use of low-cost devices in the complementary optical fibers which add to the cost. The standard sizes of large-core optical givers are 62.5/125 micrometers, 85/125 micrometers and 100/140 micrometers. There is as yet no common view on this between the two international standardization organizations concerned in the matter, the CCITT and the International Electrotechnical Commission (IEC). Because of the constant improvement in recent years in wideband (ISDNs and in single-mode optical fibers and devices, there has been a trend to the selection of single-mode optical fibers in subscriber networks. There is also the possibility of wavelength division multiplexing so that different wave lengths can use the same length of optical fiber for bidirectional transmission, thereby lowering the cost some. This is currently in the stage of continual development.

Conclusion

The foregoing discussion was concerned solely with wired media, but in certain situations it could be more economical to use radio transmissions such as microwave (analog or digital) and very high frequency. For example, the authors of item 13 in the references have demonstrated that in situations where there is no need for intermediate relays, microwave is less costly than optical fiber at distances of more than 10 km. This is especially the case where the terrain makes laying the cable difficult.

References

1. CCITT Rec., p 72, "Measurement of Reference Equivalents and Relative Equivalents." Red Book, Vol V, 1985, Geneva.

2. Tang Shuzhan [0781 3219 3277]: "An Economic and Technical Comparison of the Use of Optical Fiber Communications Systems in Local Telephone Networks." DIANXIN KEJI QINGBAO [TELECOMMUNICATIONS TECHNOLOGY INFORMATION] No 4, 1986 pp 1-9.

3. F. Hayashi, M. Iwazaqi and M. Tokuoka, "Far - End Crosstalk Properties of Dependency on Disturbing Pairs and on Cable Length." 30th IWCS Proceedings. 1981, pp 174-177.

4. J.J. Refi, "Power-sum Crosstalk of PIC Cable as a Function of Cable Design." 31st IWCS Proceedings. 1982, pp 237-244.

5. Y. Peltier, "Measures sur cable par impulsion." S.E.E.-JOURNEE D'ETUDES, 12 December 1979.

6. CCITT, "Compendium of Cable Measurement Methods." Chapters 3, 4. 1984.

7. G. Dufour, "Field Testers for Assessing 1.5 and 2.0 Mb/s Digital Performance of Metallic Pair Cable." 31st IWCS Proceedings. 1982, pp 122-130.

8. M. Balas, "Dimensioning of Digital Links Realized on Symmetric Pair Cables." BUDAVOX TELECOMMUNICATION REVIEW, 1987/3, pp 29-32.

9. CCITT, COMXV-1E, December 1984.

10. CCITT, Rec.G.613, Red Book, Vol III, Fascicle III.2, 1985, Geneva.

11. CCITT, COMXV-R7, Annex 3, July 1985.

12. CCITT, COMXV-R20, Annex 1, October 1986.

13. P. Polishuk, R. Guenther and J. Lawlor, "Cost-Comparion of Microwave, Satellite and Fibre-Optic Systems," ITU TELECOMMUNICATION JOURNAL, Vol 54, No 2, 1987, pp 114-122.

12625/7310

Automatic Monitoring/Supervisory System for Satellite Communications Networks

40080184 Beijing JISUANJI SHIJIE [CHINA COMPUTERWORLD] in Chinese No 26, 6 Jul 88 p 1

[Text] China's first independently developed multifunctional "Satellite Communications Network Automatic Monitoring System" using microcomputer automatic testing was technically certified on 9 June in Beijing by the Signal Corps Department of the [PLA] General Staff. This system was developed by satellite communications earth station technical personnel from a unit of the General Staff and is critical equipment for the central station of China's "Geosynchronous Satellite Engineering" Communications Subsystem. Its functions include on-course testing of all communications satellite transmitters, routine operational monitoring and supervision for satellite communications networks, and network entry, verification, and testing for satellite communications earth stations during the space-entry phase.

Since this system was first put into operation in May 1986 at the General Staff unit's Satellite Communications Earth Station Monitoring & Supervisory Center, it has been used for major tests involved with 12 Chinese launches of the Dong Fang 122 and Dong Fang 122A communications satellites. These tasks include orbital testing, monitoring and supervision of geosynchronous satellite communications networks, and network-entry verification at several military-base earth stations. The system has provided a great quantity of valuable and reliable data for the development and production of China's communications satellites, for communications testing, quality control, fault analysis, etc.

Because the vast majority of items involved in the system's three [principal] functions were automatically tested via microcomputer, the hand testing, data recording, charting, tabulation and other technical report responsibilities that previously required the services of 6-10 men for 15 days now can be completed by 3 men in 5 days; work efficiency and the degree of system automation have been noticeably raised. In addition, the building-block lap joints make for a flexible system construction; its functions can be easily expanded.

As revealed by the China Broadcast Satellite Company, this system's functions--except for satellite telemetry and remote control--are similar to those of the monitoring station manufactured by the Japanese Intelsat member

Yamaguchi; system precision is identical. Under conditions of similar performance, investment for this system's equipment only comes to one third that of the foreign system.

Specialists consider it to be China's first high-quality, fully functional satellite communications network automatic monitoring station. It is a major contribution to national economic construction and to the development of satellite communications.

Ministry Plans To Improve Telecommunications

[Editorial Report] Beijing RENMIN RIBAO [PEOPLE'S DAILY] (Overseas Edition) of 21 Jul 88 carries on page 3 a 450-word article detailing plans of the Ministry of Posts & Telecommunications for improving domestic telecommunications (see report from Beijing CHINA DAILY in English in FBIS-CHI-88-144, 27 Jul 88, pp 43-44). The article contains the following passage, covering material not in the aforementioned report:

"In the area of telephone switchboards, the DS-2000 program-controlled municipal telephone automatic switching system has been developed [domestically], and certification of the JD-1024[-line] program-controlled long-distance system [see JPRS-CST-88-012, 12 Jul 88, p 111] will represent a major breakthrough for China's posts & telecommunications science & technology. We are now carrying out industrial testing [of the system]. In the area of satellite communications, we have independently developed and produced 6-m and 11.6-m satellite communications earth stations, and have put them into operation. In the area of microwave technology, we have developed and produced equipment for DS 3[34 Mb/s]-and-below digital microwave systems, as well as digifax-compatible 960-line/480-line microwave system technology, which provides a medium for transforming analog microwave [systems]. In the area of fiber-optic communications, domestic development and production of equipment for fiber-optic communications systems--fiber-optic pulling apparatus, optical components, optical cable, optical terminals, optical repeaters, electronic terminals, and complete sets of instruments--have seen great advances."

40080180 END